NOAA Technical Report NOS 76 NGS 11

The Application of Multiquadric Equations and Point Mass Anomaly Models to Crustal Movement Studies

Rolland L. Hardy

Rockville, Md.
November 1978

U.S. DEPARTMENT OF COMMERCE
National Oceanic and Atmospheric Administration
National Ocean Survey

NOAA Technical Publications

National Ocean Survey/National Geodetic Survey subseries

The National Geodetic Survey (NGS) of the National Ocean Survey (NOS), NOAA, establishes and maintains the basic National horizontal and vertical networks of geodetic control and provides governmentwide leadership in the improvemment of geodetic surveying methods and instrumentation, coordinates operations to assure network development, and provides specifications and criteria for survey operations by Federal, State, and other agencies.

NGS engages in research and development for the improvement of knowledge of the figure of the Earth and its gravity field, and has the responsibility to procure geodetic data from all sources, process these data, and make them generally available to users through a central data base.

NOAA Technical Memorandums and some special NOAA publications are sold by the National Technical Information Service (NTIS) in paper copy and microfiche. Orders should be directed to NTIS, 5285 Port Royal Road, Springfield, VA 22161 (telephone: 703-557-4650). NTIS customer charge accounts are invited; some commercial charge accounts are accepted. When ordering, give the NTIS accession number (which begins with PB) shown in parentheses in the following citations.

Paper copies of NOAA Technical Reports, which are of general interest to the public, are sold by the Superintendent of Documents, U.S. Government Printing Office (GPO), Washington, D.C. (telephone: 202-783-3238). For prompt service, please furnish the GPO stock number with your order. If a citation does not carry this number, then the publication is not sold by GPO. All NOAA Technical Reports may be purchased from NTIS in hard copy and microform. Prices for the same publication may vary between the two Government sales agents. Although both are nonprofit, GPO relies on some Federal support whereas NTIS is self-sustained.

An excellent reference source for Government publications if the National Depository Library program, a network of about 1,300 designated libraries. Requests for borrowing Depository Library material may be made through your local library. A free listing of libraries currentlty in this system is available from the Library Division, U.S. Government Printing Office, Arlington, VA 22304 (telephone: 703-557-9013).

NOAA Geodetic publications

Classification, Standards of Accuracy, and General Specifications of Geodetic Control Surveys. Federal Geodetic Control Committee, John O. Phillips (Chairman), Department of Commerce, NOAA, NOS, 1974 reprinted annually, 12 pp (PB265442). National specifications and tables show the closures required and tolerances permitted for first-, second-, and third-order geodetic control surveys.

Specifications To Support Classification, Standards of Accuracy, and General Specifications of Geodetic Control Surveys. Federal Geodetic Control Committee, John O. Phillips (Chairman), Department of Commerce, NOAA, NOS, 1975, reprinted annually 30 pp (PB261037). This publication provides the rationale behind the original publication, "Classification, Standards of Accuracy, ..." cited above.

NOAA Technical Memorandums, NOS/NGS subseries

NOS NGS-1 Use of climatological and meteorological data in the planning and execution of National Geodetic Survey field operations. Robert J. Leffler, December 1975, 30 pp (PB249677). Availability, pertinence, uses, and procedures for using climatological and meteorological data are discussed as applicable to NGS field operations.

NOS NGS-2 Final report on responses to geodetic data questionnaire. John F. Spencer, Jr., March 1976, 39 pp (PB254641). Responses (20%) to a geodetic data questionnaire, mailed to 36,000 U.S. land surveyors, are analyzed for projecting future geodetic data needs.

NOS NGS-3 Adjustment of geodetic field data using a sequential method. Marvin C. Whiting and Allen J. Pope, March 1976, 11 pp (PB253967). A sequential adjustment is adopted for use by NGS field parties.

NOS NGS-4 Reducing the profile of sparse symmetric matrices. Richard A. Snay, June 1976, 24 pp (PB-258476). An algorithm for improving the profile of a sparse symmetric matrix is introduced and tested against the widely used reverse Cuthill-McKee algorithm.

NOS NGS-5 National Geodetic Survey data: availability, explanation, and application. Joseph F. Dracup, June 1976, 45 pp (PB258475). The summary gives data and services available from from NGS, accuracy of surveys, and uses of specific data.

(Continued at end of publication)

NOAA Technical Report NOS 76 NGS 11

The Application of Multiquadric Equations and Point Mass Anomaly Models to Crustal Movement Studies

Rolland L. Hardy

National Geodetic Survey
Rockville, Md.
November 1978

U.S. DEPARTMENT OF COMMERCE
Juanita M. Kreps, Secretary

National Oceanic and Atmospheric Administration
Richard A. Frank, Administrator

National Ocean Survey
Allen L. Powell, Director

CONTENTS

THE APPLICATION OF MULTIQUADRIC EQUATIONS AND POINT MASS ANOMALY MODELS TO CRUSTAL MOVEMENT STUDIES

Rolland L. Hardy*
National Geodetic Survey
National Ocean Survey, NOAA,
Rockville, Md. 20852

ABSTRACT. The basic theory of multiquadric (MQ) equations relevant to crustal movement studies is summarized. Both the hyperboloid and reciprocal hyperboloid kernels of an MQ function are given a point mass anomaly interpretation. They are applied to a realistic "error-free" model of subsidence in the Houston-Galveston area, in a pure prediction test. The standard error of a single prediction was found to be less than 0.5 cm/yr for optimum depths of point mass anomalies, using either the hyperboloid or reciprocal hyperboloid as kernels. The rectangular study area of about 88 by 124 km included 49 "error-free" sample points in an irregular pattern, and 49 "error-free" prediction points in a grid pattern. Subsidence rates in the area ranged from about -1 cm/yr to -9 cm/yr. Only subsidence information provided by geodetic leveling (simulated) was used.

Geophysical interpretation beyond developing the point mass anomaly model was somewhat limited. Future tests should include details of the gravity anomalies and topography to determine the full potentiality and limitations of point mass models for interpreting the mass redistribution associated with crustal movement.

MULTIQUADRIC EQUATIONS

Multiquadric equations have been applied in the past to topography, gravity anomalies, hydrologic studies, magnetic anomalies, terrain corrections, world geoid determination, geologic subsurface studies, and photogrammetry, including image reconstruction. This publication, together with a concurrent paper coauthored with Sandford Holdahl (Holdahl and Hardy 1977) of the National Ocean Survey (NOS) National Geodetic Survey (NGS), is the first report of studies applying MQ equations to crustal movement.

The background information provided in this section is designed to familiarize the reader with the many flexible features of MQ equations. This is a

*Prepared during a five-month grant period as a Senior Scientist in Geodesy, National Research Council, National Academy of Sciences, Washington, D.C., while on leave from Iowa State University, Ames, Iowa.

condensed version of previous publications, and includes additional insights into point mass anomaly methods. New ideas concerning the relationship of MQ functions to deterministic covariance functions are presented. Novel concepts involving "mascon anomalies" and isostatic trends of MQ functions are described. It also shows that a variation of the fictitious observation equations as used in least-squares adjustment can be used for least-squares prediction.

The basic hypothesis of MQ analysis is that any smooth mathematical surface and also any smooth irregular surface (mathematically undefined) may be approximated to any desired degree of exactness by the summation of regular, mathematically defined surfaces, especially displaced quadric forms. "Displacement" in this case roughly corresponds to "lag" in a time series, although the analogy is by no means exact. MQ equations in Cartesian coordinates may, in general, be represented by

$$\sum_{j=1}^{n} \alpha_j Q(X, Y, X_j, Y_j) = f(X, Y) = Z \tag{1}$$

where the α_j's are undetermined coefficients, and each $Q(X, Y, X_j, Y_j)$ is a quadric kernel function of X and Y, centered at coordinates X_j, Y_j. The ordinates Z of the complete function f(X, Y) are determined by the summation (superposition) of many quadric kernels, hence "a multiquadric (MQ) function" (Hardy 1971).

A frequently used example of a quadric kernel is the hyperboloid

$$Q(X, Y, X_j, Y_j) = \left[\left(X - X_j\right)^2 + \left(Y - Y_j\right)^2 + \delta^2\right]^{1/2} \tag{2}$$

where δ is usually interpreted in geometric terms alone as the perpendicular distance from the X, Y plane to the hyperbolic minimum. The hyperboloid kernel has a fairly remarkable relationship with its reciprocal

$$Q(X, Y, X_j, Y_j) = \left[\left(X - X_j\right)^2 + \left(Y - Y_j\right)^2 + \delta^2\right]^{-1/2}. \tag{3}$$

In this case, δ can be interpreted as the perpendicular distance of a unit point mass (or point mass anomaly) from the X, Y plane on which the potential (or disturbing potential) is evaluated. Consequently, two general branches (harmonic and nonharmonic) can be developed from eqs. (1), (2), and (3).

For disturbing potential (T) and other harmonic phenomena with respect to a plane, the basic logical form is

$$G \sum_{j=1}^{n} \alpha_j \left[\left(X - X_j\right)^2 + \left(Y - Y_j\right)^2 + \delta^2 \right]^{-1/2} = T. \tag{4}$$

Note that the universal constant of gravitation precedes the summation. The coefficients δ_j now take on the proper dimension and interpretation of point mass anomalies with respect to standard point masses in the model.

For topography and other nonharmonic phenomena with respect to a plane, the basic logical form is

$$\frac{G}{K} \sum_{j=1}^{n} \alpha_j \left[\left(X - X_j\right)^2 + \left(Y - Y_j\right)^2 + \delta^2 \right]^{+1/2} = H \tag{5}$$

where H, representing topography, has been substituted for the dependent variable Z. It is appropriate to give the symbols G, α_j, and δ in eq. (5) the same interpretation as in eq. (4) because the theory of isostasy connects these equations in a conceptual way. For this reason, a constant K has also been introduced. This will be discussed in more detail later.

Equations (4) and (5) are transformable to spherical coordinates by noting that δ (depth with respect to a plane) can be visualized as a quantity (R-r), i.e., the radial difference between two spheres with the same origin. Then for every point mass anomaly at r_j, θ_j, λ_j on the inner sphere r, there is a radially corresponding R_i, θ_i, λ_i on the outer sphere R. Conceptually, we can visualize an infinitely large set of Cartesian coordinates X, Y, Z as the locus of evaluation points on sphere R, including a finite set R_i, θ_i, λ_i. Similarly, an infinitely large set of Cartesian coordinates X_j, Y_j, Z_j can

exist on sphere r, including the finite set r_j, θ_j, λ_j. This conception justifies the substitution of $(Z-Z_j)^2$ for δ^2 in eqs. (4) and (5). Then T and H are functions of the three variables, f(X, Y, Z). A transformation of eq. (4) to spherical coordinates results in

$$G \sum_{j=1}^{n} \alpha_j \left[R^2 + r^2 - 2Rr \cos\psi_j\right]^{-1/2} = T \tag{6}$$

where

$$\cos\psi_j = \cos\theta \cos\theta_j + \sin\theta \sin\theta_j \cos(\lambda - \lambda_j).$$

The radius r is not subscripted at this point, and is taken as the optimum constant radius of the inner sphere. The formula for the best constant r (Hardy and Göpfert 1975) will be given later.

Equation (5) is similarly transformable, resulting in

$$\frac{G}{K} \sum_{j=1}^{n} \alpha_j \left[R^2 + r^2 - 2Rr \cos\psi_j\right]^{1/2} = H \tag{7}$$

where H represents topographic ordinates with respect to a sphere.

The formulation of a linear system of equations and the solutions for the undetermined coefficients in eqs. (4), (5), (6), and (7) all follow the same pattern. This is also true for any new relationships that may be derived from them. For example, Hardy and Göpfert (1975) have already derived particular MQ relationships from eq. (6) that express geoidal undulations N, components of the deflections of the vertical ξ and η, gravity anomalies Δg, and gradients of the gravity anomaly $\partial(\Delta g)/\partial R$. Consequently (with $K = \gamma$, $K = 1$, or any other appropriate constant), we may express an MQ system of linear equations in a general form as

$$\frac{G}{K} \sum_{j=1}^{n} \alpha_j Q_{ij} = \zeta_i \qquad i = 1, 2, 3...m, \; m \geq n \tag{8}$$

where the symbols G and α_j are still the same as previously defined. The symbol Q_{ij} represents any particular quadric kernel, appropriately related in a geometric and physical sense to the measurements ζ_i. The subscript pair ij refers to the location of the i'th data point, and the location (node) of the j'th kernel. These subscripted kernels form the coefficient matrix of the observation equations. The kernel functions can be in either plane of spherical coordinates, and either harmonic or nonharmonic in their physical interpretation. The symbol ζ_i indicates a column list of data ordinates such as N_i, Δg_i, H_i, ξ_i, η_i, etc. The equivalent of eq. (8) in matrix notation for observation equations is

$$\frac{G}{K} \left[Q_{ij}\right] \left[\alpha_j\right] - \left[\zeta_i\right] = \left[V_i\right] \qquad \begin{matrix} i = 1, 2, 3... \; m \\ j = 1, 2, 3... \; n, \; m \geq n \end{matrix} \tag{9}$$

where the V_i's are residuals.

When m = n, a unique solution is found. For the more general case, with m > n, the least-squares solution for the product of K^{-1}, the universal constant of gravitation G, and the coefficients is

$$\frac{G}{K} \left[\alpha_j\right] = \left[\left(Q_{ij}\right)^T \left(Q_{ij}\right)\right]^{-1} \left[\left(Q_{ij}\right)^T \left(\zeta_i\right)\right]. \tag{10}$$

For an analysis of the prediction error, we can determine ΣV^2 with

$$V^T V = \left[Q(Q^T Q)^{-1} (Q^T \zeta) - \zeta\right]^T \left[Q(Q^T Q)^{-1} (Q^T \zeta) - \zeta\right] \tag{11}$$

in which the subscripts have been omitted.

Then the least-squares prediction of a column vector of $\tilde{\zeta}_p$'s is

$$\left[\tilde{\zeta}_p\right] = \left[Q_{pj}\right] \left[\left(Q_{ij}\right)^T \left(Q_{ij}\right)\right]^{-1} \left[\left(Q_{ij}\right)^T \left(\zeta_i\right)\right]. \tag{12}$$

For the unique case, i.e., m = n, which is the limiting case of least squares, eq. (12) for a single $\tilde{\zeta}_p$ reduces to

$$\tilde{\zeta}_p = \left[Q_{pj}\right] \left[Q_{ij}\right]^{-1} \left[\zeta_i\right]. \tag{13}$$

We note that eq. (13) is the equivalent of the least-squares prediction formula given by Heiskanen and Moritz (1967, p. 268) for covariance functions. However, Q_{ij} is, in general, not required to be a covariance kernel corresponding to C_{ik} of Heiskanen and Moritz (Hardy 1976, 1977). The hyperboloid kernel, with no statistical meaning or stochastic interpretation, is a good contrary example. On the other hand, the reciprocal hyperboloid and its spherical counterpart do qualify as deterministic covariance functions, i.e., these functions satisfy the geometric requirements of a covariance function as given in Yaglom (1962, p. 24), but without regard for a random process interpretation. Moreover, the underlying reality of eq. (4) and its spherical counterpart (Hardy and Göpfert 1975) is that they are intrinsically related to Newton's laws, and are therefore deterministic. In this case, deterministic means not only routinely solvable (nonsingular coefficient matrix), but that the output is completely determined in a physical sense for a given input (Miller 1963, p. 285).

There is another justification for asserting that some MQ functions qualify as deterministic covariance functions. As shown by Heiskanen and Moritz (1967), the covariance function $C(\psi)$ can be expanded in Legendre polynomials in the form

$$C(\psi) = \sum_{n=2}^{\infty} c_n P_n (\cos \psi). \tag{14}$$

If $C(\psi)$, as given above, is appropriate for geoidal undulations, then the c_n's must be degree variances for the geoid. Thus, we can express a corresponding linear system of covariance equations as

$$N_i = \sum_{j=1}^{n'} \beta_j C(\psi_{ij}) = \sum_{j=1}^{n'} \beta_j \sum_{n=2}^{\infty} c_n P_n(\cos \psi_{ij}) \quad i = 1, 2 \ldots m, \; m \geq n' \qquad (15)$$

where n' is the total number of covariance kernels, and n gives the degree of each Legendre polynomial. The undetermined coefficients are designated as β_j in this case because, in general, they do not have the point mass anomaly interpretation, as given to the α_j's, in the MQ harmonic method.

If the coefficients c_n were found deterministically, eq. (15) could be called a deterministic covariance function because the polynomials $c_n P_n (\cos \psi)$ would be directly related to Newton's laws, and not depend on stochastic processes. In other words, there are deterministic as well as stochastic models in developing and using covariance functions, but the distinction is seldom made clear in contemporary literature.

Empirical covariance kernels for eq. (15) are frequently developed directly from geoidal undulations in a stochastic process model

$$C(\psi) = M\{N \cdot N'\} \; , \qquad (16)$$

i.e., $C(\psi)$ is said to be a function equal to the mean of a set of products $N \cdot N'$ over a sphere, where all N and N' are geoidal undulations separated by spherical distances ψ that are consecutively specified varying from zero to π. Formal integral formulas are frequently given, but they must be solved by numerical summation with discrete samples.

An alternate approach is to use tabulated degree variances c_n, previously determined by a stochastic estimate. These are substituted for c_n (up to a truncation level) in the Legendre polynomial equivalent of $C(\psi)$, also modeled in eq. (15). In both cases, the approach involves stochastic processes either directly or indirectly.

We can now illustrate a finite deterministic form of the covariance function by expanding each MQ kernel in eq. (4), and its spherical counterpart (Hardy and Göpfert 1975, eq. (5)) into an infinite series of plane and spherical Legendre polynomials respectively. The spherical form becomes

$$T = G \sum_{j=1}^{n'} \alpha_j \sum_{n=2}^{\infty} \frac{r^n}{R^{n+1}} P_n (\cos \psi_j) \tag{17}$$

where r is the radius of an inner sphere on which the point mass anomalies are located, and R is the mean radius of the Earth.

Using Bruns' formula $T = N\gamma$ and forming a linear system of equations as in eq. (15), we have

$$N_i = \sum_{j=1}^{n'} \alpha_j \sum_{n=2}^{\infty} \frac{G}{\gamma} \frac{r^n}{R^{n+1}} P_n (\cos \psi_{ij}) \quad i = 1, 2...m, \; m \geq n'. \tag{18}$$

Now we can see that the MQ harmonic function, as developed in this report, is the equivalent of a very special case of covariance functions, i.e., a purely deterministic case. Equation (15) is identical to eq. (18) for the case $\beta_j = \alpha_j$ in which the undetermined coefficients are point mass anomalies, provided also that the degree variances are simultaneously

$$c_n = \frac{G}{\gamma} \frac{r^n}{R^{n+1}} . \tag{19}$$

Some modification of eq. (19) and further comment are appropriate because the optimum inner radius r is determinable with the best-r formula previously mentioned. Letting δ represent the variable depth of point mass anomalies, then $\delta = R - r$, and eq. (19) becomes

$$c_n = \frac{G}{\gamma R} \left(1 - \frac{\delta_o}{R}\right)^n \tag{20}$$

where δ_o is the optimum depth of point mass anomalies, as determined from the best-r formula. Thus, the c_n's in eq. (20) are optimum, deterministic degree variances, containing two physical parameters (G and γ) and two geometric parameters (δ_o and R). Stochastic processes were irrelevant in their determination. The next paragraph will explain why the difference between deterministic and stochastic degree variances is an important distinction.

The contemporary use of the covariance kernel in eq. (15) is deficient because the coefficients c_n in the kernel are, as previously mentioned, directly or indirectly estimated by a principle involving stochastic processes on a sphere. Lauritzen (1973) has called attention to this deficiency on highly theoretical grounds pointing out that a Gaussian random field on a sphere is not ergodic. Consequently, sample averages over a sphere cannot rigorously determine an apparent covariance function or degree variances. According to Lauritzen (1973, p. 80), "...the problem is not suited for statistical treatment...."

MQ analysis avoids this difficulty by being more explicit in a deterministic sense, particularly concerning a point mass model. Hardy (1976, 1977) has previously shown that for MQ harmonic analysis, determining apparent or empirical covariances in a stochastic sense is irrelevant. Moreover, Hardy and Göpfert (1975) made a remarkable and practical confirmation of Lauritzen's theoretical point of view in deriving the best-r formula. In deriving this formula, which is equivalent to determining the optimum depth of point mass anomalies, the solution was completely independent of the data ordinates N. Instead, the best-r (optimum δ_o) was dependent almost exclusively on the average spacing of data ordinates, and not on the magnitude of ordinates or averaging of lagged ordinate pairs over a sphere.

To conclude our comments on covariance functions, we will justify using MQ equations instead of expanding them into Legendre polynomials for discrete data as used in eq. (17) for illustrative purposes. The reasoning is slightly indirect, but not difficult. First, to reduce a problem involving discrete data to an optimum point mass anomaly model for the solution

involves making a simplified or engineering-type assumption. This assumption helps solve the problem in a relatively simple manner, and implies the willingness to accept a result that will not be the same as for a more complete and accurate data set. Moreover, it enables one to get the most out of the available discrete data without obscuring the basic physical meaning of the results. In any case, having made this a priori decision, it is better to use a simple method that responds exactly to Newton's laws for a given input of discrete data than to substitute a more complicated, infinite Legendre series for the computation. Such a substitution not only compounds the computational aspect, but it also involves an additional approximation because of the necessary truncation of the series. Perhaps an exception to this line of reasoning could be made if it were actually possible to use the orthogonal polynomial properties of the Legendre series to determine coefficients or degree variances unambiguously by formal and exact integration. Generally, in practice, this is not the case. So the application of a multiquadric series to a discrete data problem, reducible to an optimum point mass anomaly problem as shown above, will probably be superior to other contemporary methods regarding the following features:

1) accuracy of the solution,
2) computational efficiency, and
3) physical interpretation of the results.

Item 3 in this list has been the basis for studying the apparent isostatic response of eq. (7), based on coefficients (point mass anomalies) determined from a variation of eq. (6). It has been previously shown (Hardy and Göpfert 1975) that the coefficients determined from one type of MQ series can be substituted into any other appropriate MQ series for prediction purposes. Thus, for example, geoidal undulations $\tilde{N}_p$ can be predicted from

$$\tilde{N}_p = \frac{G}{\gamma} \sum_{j=1}^{n} \alpha_j \left[R^2 + r^2 - 2Rr \cos \psi_{pj} \right]^{-1/2} \qquad p = 1, 2, 3... \qquad (21)$$

when the coefficients α_j have been solved from a linear system of equations

$$G \sum_{j=1}^{n} \alpha_j \left[\frac{R - r \cos \psi_{ij}}{\ell_{ij}^2} \frac{2}{\ell_{ij} R} \right] = \Delta g_i \qquad i = 1, 2 \ldots m, m \bar{>} n \tag{22}$$

in which

$$\ell_{ij} = \left(R^2 + r^2 - 2Rr \cos \psi_{ij} \right)^{1/2} .$$

Equation (21) is a simple variation of eq. (6), obtained by substituting $N\gamma$ for T (Bruns' formula). It is also the basic MQ form for expansion into a linear system of Legendre polynomial equations as given in eq. (18). Equation (22) is a linear equation expansion of a basic MQ series derived from eq. (6). The left hand side of eq. (6) and its derivative $\partial T/\partial R$ are substituted into one of the basic forms of the fundamental equation of physical geodesy, namely $\Delta g = -\partial T/\partial R - 2T/R$.

By analogy, the implication is also present that predictions of H_p can be made with eq. (7), provided the coefficients α_j are determined from a linear system of equations, such as

$$\frac{G}{\gamma} \sum_{j=1}^{n} \alpha_j \left[R^2 + r^2 - 2Rr \cos \psi_{ij} \right]^{-1/2} = N_i \qquad i = 1, 2 \ldots m, m \bar{>} n. \tag{23}$$

In this case, the mathematical relationship is simpler. The kernel functions in eqs. (7) and (23) are merely reciprocals of each other, and K replaces γ, but the physical interpretation is more difficult. The validity of the relationship between the two equations is not immediately obvious. Equation (7) involves topographic heights which are generally a nonharmonic phenomenon. The relatively clear relationship of gravity anomalies to geoidal undulations, based exclusively on potential theory, is not present in the possible relationship of topographic heights to geoidal undulations. Consequently, we must consider other or indirect effects that would somehow relate topographic heights to point mass anomalies. One possibility for consideration is the theory of isostasy. This theory is based on the existence of

some form of mass deficiency under topographic highs and mass excesses under topographic lows (bathymetry or ocean bottoms).

A few check computations with a global model have confirmed that the function for H in eq. (7) does indeed tend toward positive values in regions dominated by negative point mass anomalies as determined from the system in eq. (23). For regions of predominately positive anomalies, the geoid from eq. (23) tends to rise appropriately, whereas H in eq. (7) tends to subside to negative values. Thus, the topographic heights in this case are not at all related to the Molodenski-type height anomaly, which tends to have the same algebraic signs and magnitudes as the geoidal undulations N. Instead, eq. (7) modulates the topography in close agreement, frequency-wise, with isostatic tendencies indicated by contemporary theories of isostasy. The appropriate amplitude modulation of the topography computed from eq. (7) is dependent on the magnitude of the constant K, however; a detailed rigorous computation of this constant has not yet been developed. It is beyond the objectives of this report to develop a complete isostatic model, which would involve several refinements of the MQ method for determining point mass anomalies. We will only suggest a direction future investigations should take in developing such a model.

Equation (7) does not appear to include the influence of the Earth's density, but this effect may be considered to be a part of the constant K. This is only one of several effects that should be considered in the computation of this factor. It is among the most important, and other effects will depend upon it. An extension of the concept of a point mass anomaly to a representative volume distribution of the mass anomaly is undoubtedly necessary. In this report we have been careful to use the expression "point mass anomaly" rather than "point mass." Hence, the mass anomalies that sum to zero have already been superimposed upon the interior of a spherical approximation of a Standard Earth Model. It appears now that our Standard Earth Model should include a density profile up to the crust-mantle boundary at least, in addition to the usual Geodetic Reference System.

In the context of a point mass anomaly, negative does not mean less than zero mass. It means less than a normal mass, with respect to some standard mass distribution that is intrinsically positive. The point mass anomaly is initially associated with the point location of the anomaly at the best-r value (optimum δ_o). In combination with a proper volume for the mass anomaly, it is easy to perceive that buoyancy with a fluid Earth of variable density will provide the basis for the rise or fall of a mass anomaly to a position of equilibrium above or below the best r, thus physically confirming the indication of an isostatic trend. Determining the proper scale factors for propagation and amplification of this effect at the crustal surface requires considerably more analysis than can be accomplished here. Nevertheless, we have introduced the key concept of "mascon anomaly," which can be either negative or positive, to incorporate a density model in the computation of the constant K in eq. (7). This is a simple modification of the concept of a mascon, ordinarily used with only a positive definition.

During the future development of the theoretical details for complete quantification of the isostatic trends represented by eq. (7), we must remember the contemporary difficulties with all isostatic models. The "real" Earth almost never conforms with any isostatic model to a degree of precision consistent with the idealization frequently used to simplify the computations. This will doubtlessly be true also of the MQ approach to an isostatic theory. Nevertheless, an earlier, almost completely heuristic interpretation of the hyperboloid kernel as being deterministically suitable for topography (Hardy 1972) is being supported theoretically and practically in an unusual way. As with point mass and material surface methods in general, "...This case is more or less fictitious but it nevertheless is of great theoretical importance." (Heiskanen and Moritz 1967, p. 5.)

During the preceding presentation, we have frequently referred to the best-r formula, sometimes indirectly by comments on an optimum radius or optimum depth of point mass anomalies. The parameter r was introduced in eq. (6) and defined as the optimum constant radius of an inner sphere on which point mass anomalies are located. We will now discuss the methods of determining the best-r, including the best-r formula (Hardy and Göpfert 1975; Hardy 1976).

The radius r in a system of equations, as in eq. (23) for example, was treated originally as an unknown in addition to the undetermined coefficients α_j, making the system nonlinear. When this is done, the number of observation equations is one less than the number of unknowns, provided we center an MQ kernel at every observed data ordinate N_i. For maximum use of observed data, an MQ kernel was used at every observed data ordinate; the formation of fictitious observation equations easily removed the deficiency in the number of equations.

The validity of this aspect of the solution was not discussed thoroughly in the otherwise complete derivation of the best-r formula by Hardy (1976). We will now discuss fictitious observation equations, as applied to least-squares prediction, in greater detail than in any previous report.

For background information, we note that fictitious observations equations are already an accepted procedure in least-squares adjustment, in contrast with least-squares prediction. According to Hirvonen (1971), fictitious observations are often used in least-squares adjustment to reduce the number of observations in a highly overdetermined system. A single functional observation replaces a number of observed quantities by subdividing a large problem into smaller parts that can be solved more routinely. In preprocessing a group of observations of the larger problem into a single representative observation, i.e., a fictitious observation, it is essential to use the statistical properties of the weighted mean of the group. A simple example of a fictitious observation is to replace the several observed angles at a traverse station with a single mean value which is used in the subsequent traverse adjustment.

In least-squares prediction with MQ functions, a minor variation of this same basic principle can be used. The prediction problem may be viewed as one involving a finite sample of ordinates from an indefinitely large prediction vector. The problem is to find a solution that is optimum in some sense, even though the system of equations for doing so is underdetermined (Moritz 1976). An empirical covariance kernel function is one least-squares method of optimizing an underdetermined system, but it is not the

only method. In fact, redundancy may be present in all of the computational aspects of least-squares prediction with MQ functions. In some cases the fictitious observation concept of least-squares adjustment may be directly applicable to a part of the problem without modification.

Consider, for example,a set of observations of the ordinate or other measurable quantity at a single geographic location. Obviously, a single most probable value determined from either a weighted or simple mean, according to circumstances, may be substituted for the larger set. Generally, nothing will be lost in a least-squares adjustment by making this substitution, and some gain in computational efficiency can result from it. Generally, if least-squares prediction is somehow dependent on the set of observations rather than each observation by itself, nothing can be gained by forming observation equations for each separate observation in lieu of the single mean, and to do it will decrease computational efficiency. Theoretically it is valid to form an equation for each observation, but it is not useful. On the other hand, the mean anomaly concept, as mentioned above, has an exceptional property which may be applied in a useful manner to either least-squares adjustment or least-squares prediction.

The theoretical justification for using mean anomalies in least-squares prediction with MQ functions is rather unique; an expansion of the number of observation equations is merely a useful byproduct. A mean anomaly is numerically equal to the weighted mean of several ordinates at different locations, and in this respect is very similar to the mean of several ordinate observations at the same location, as in the preceding paragraph. This is not a complete definition however. We must specify the single point location as well as the magnitude of a mean anomaly to make appropriate use of it. Generally, a single point location for a mean anomaly is the center of a block or other regular figure represented by the anomaly. This point location is generally not coincident with any of the separately observed ordinates. In any case, a discrete mean anomaly cannot occupy the point location of more than one of the single ordinates in the set or group, and even this possibility can be eliminated by an appropriate choice of regional boundaries.

Thus, under certain conditions, an MQ least-squares prediction method on a sphere may be composed of two parts; one part minimizes the sum of the squares of the residuals at all observed data ordinates making use of real observation equations; the other part minimizes the sum of the squares of the residuals at the estimated regional mean anomaly ordinates (a single ordinate for each region), making use of fictitious observation equations. The justification for using fictitious observation equations, which are consistent with predictions of the mean regional anomalies, is fundamentally the same as for estimating the mean of a set of observations in the preprocessing commonly associated with least-squares adjustment. In the case of least-squares adjustment there is a decrease in the number of observation equations, which is computationally efficient. In the case of least-squares prediction there can be an increase in the number of observation equations. Ordinarily this is not computationally efficient, but it will be useful if one is enabled to get a routine solution of an otherwise underdetermined system of equations. The usefulness becomes particularly noteworthy when the real observation equations by themselves fail to give continuous predictions of regional anomalies that are consistent with the mean of discrete data in each region.

To illustrate the point we will consider an alternative approach to solving the system of equations in eq. 23. Using n observed geoidal ordinates on a sphere, and n MQ kernels, we may obtain a unique solution for n undetermined coefficients α_j, provided any arbitrary finite value for the radius r (except r=0 or r=R) is assigned in advance. This is equivalent to an assumption that there is no rational method of determining the best-r either a priori, or as part of the solution for the α_j's. Then, in general, all such unique solutions obtained by changing r arbitrarily will fit the observed geoidal ordinates exactly except for roundoff error. On the other hand, only one of these unique predictions (the one with the best-r) will correspond to the minimization of the squares of the difference between the computed regional mean anomalies on the sphere and the predicted regional mean anomalies on the sphere. Unless an appropriate modification of the set of observation equations is made, finding the best-r remains a matter of trial and error. The real observation equations for single ordinates are, by themselves, ineffective; they do not assure

consistency between the measured and the predicted mean anomalies. The desired consistency may be assured by supplementing the real observation equations with fictitious observation equations, each of which incorporates the correlation of a set of real observations in a region with its a priori estimated (or fictitious) mean. As a by-product, the extra observation equations provide a means for determining the best-r simultaneously with the undetermined coefficients α_j in a nonlinear least-squares solution.

The principle described above was originally used to determine the best-r by least squares prediction with MQ functions. Fictitious observations were introduced with the assumption that the most probable ordinate at the midpoint of a line joining two adjacent actual ordinate observations was equal to the mean of the actual observations. This is nothing more or less than the computation of the mean anomalies for small regions having only two data points each, and placing the resulting mean ordinate at the centroid of the two-point regional data. The nonlinear least-squares system of equations based on this concept converged rapidly to give a solution for the undetermined α_j's and also the best-r. It was found later that the best-r, determined by least-squares in this way, was not significantly different from that determined by what is now called the best-r formula. This formula and related equations will be discussed in the following paragraphs.

The best-r formula resulted from a simple extension of the concept of fictitious observation equations as applied to least-squares prediction with MQ equations. In forming three real observation equations for data ordinates at the vertices of an equilateral triangle on a sphere, and adding these to a single fictitious observation for the computed mean anomaly of these three ordinates at the centroid of the same equilateral triangle, a rather remarkable relationship was discovered. A unique solution for r existed which was not dependent at all on the magnitude and algebraic sign of the ordinates at the vertices. This meant also that for any adjacent equilateral triangle, congruent with the first triangle on one side, the same unique solution for r existed without regard for the magnitude or sign of the ordinates at ends of the congruent side, nor of the ordinate at the new vertex.

In brief, the discovery rapidly expanded into the concept that there is a unique best-r for any number of data ordinates on a sphere, independent of the magnitude and sign of the ordinates, particularly if the data are regularly spaced at the vertices of nonoverlapping equilateral triangles. Consequently, MQ equations and the spherical trigononometry of equilateral triangles were used to develop the following condition equation:

$$\frac{1}{R-r} + \frac{2}{\left(R^2 + r^2 - 2Rr \cos \psi_s\right)^{1/2}} - \frac{3}{\left(R^2 + r^2 - 2Rr \cos \psi_m\right)^{1/2}} = 0 \qquad (24)$$

where all parameters have been previously defined except ψ_s and ψ_m. The symbol ψ_s represents angular length of a single side of an equilateral spherical triangle. The symbol ψ_m represents the angular distance on a sphere from a vertex of the same triangle to the surface centroid of the triangle.

Equation (24) may be solved directly for r, when n data points on a sphere of given radius R have been specified and the corresponding ψ_s and ψ_m are computed. Formulas for ψ_s as a function of n and ψ_m as a function of ψ_s are given below. The best-r formula, based on a least-squares prediction principle, is very convenient for MQ and other point mass methods. It means that the best-r can be determined before using systems of equations such as eq. (23). Consequently, linear least squares rather than iterative non-linear methods can solve all MQ systems used to date (1977). As previously mentioned, the best-r formula indicates that optimum least-squares prediction with the MQ method is not dependent on averaging ordinate pairs over a sphere, as used in autocorrelation to determine an empirical covariance kernel function. Equation (24) provides an optimum solution based only on the spacing of data ordinates, not the averaging of ordinate pairs at various distances as for empirical covariance. Thus, the theoretical difficulties described by Lauritzen (1973) are not relevant to MQ equations.

On the other hand, a potential difficulty was present because equal spacing of data or nodes cannot be made exactly on a sphere, except for special cases. However, use of the best-r formula in practice indicates

that it also works extremely well for unequally spaced data. With irregular data spacing, the computed ψ_s is a close approximation if not the exact mean side length of an array of nonequilateral, nonoverlapping triangles on a sphere. In fact, there is no significant difference in determining the best-r for irregularly spaced data by the above formula, as compared with a simultaneous nonlinear least-squares solution for r and α_j's using the same irregulary spaced data.

Useful auxiliary formulas for (24) are

$$\psi_s\ (n) = 2\ \tan^{-1}\left[1 - 2\cos\frac{\pi n}{3(n-2)}\right]^{1/2} \tag{25}$$

in which n is the number of nodes, and in turn

$$\psi_m = \tan^{-1}\left[\frac{2^{1/2}\ (1 - \cos\psi_s)}{(\cos\psi_s - \cos 2\psi_s)^{1/2}}\right] \tag{26}$$

Table 1, which lists the best-r for $10 \leq n \leq 500$, was developed using eqs. (24, (25), and (26).

For regional rather than global cases, eq. (25) becomes

$$\psi_s\ (n, A) = 2\ \tan^{-1}\left[1-2\cos\left(\frac{A}{6(n-2)\ R^2} + \frac{\pi}{3}\right)\right]^{1/2} \tag{27}$$

in which A is the area of the region on a sphere, and n is the number of nodes used in the region.

As a result of studies connected with this report, the estimate of optimum depth δ for point mass anomalies with respect to a plane as in eq. (4) can be found from

$$\frac{1}{\delta} + \frac{2}{(\delta^2 + s^2)^{1/2}} - \frac{3}{(\delta^2 + 1/3\ s^2)^{1/2}} = 0 \tag{28}$$

in which s is the length of a side of the nonoverlapping equilateral triangles (or the mean side length of nonequilateral nonoverlapping triangles) with nodal points located at the triangle vertices. This δ should also probably be used in eq. (5) for future studies involving an interaction of harmonic and nonharmonic functions. For topography and other nonharmonic phenomena alone, the following formula has been used with respect to a plane,

$$\delta = 0.665\ D^2 \tag{29}$$

where D is the rectangular grid spacing of nodes (or the equivalent mean for irregularly spaced nodes). Equation (29) was empirically developed with an MQ fit to spline functions and has not been shown to be an optimum estimate. However, it has provided workable, smoothing values for all cases encountered up to this time.

This concludes the review of MQ analysis that has had a bearing on the study of crustal movement applications to date. Future development of the method may involve such matters as hybrid data, use of the osculating surface principle, and concentric superposition of MQ functions. At the present time (1977), the most complete document on such matters is a report to the National Science Foundation, under Grant GK-40287 (Hardy 1976).

VERTICAL CRUSTAL MOVEMENT STUDIES

Studies of crustal movement provide a better understanding of Earth dynamics. Practical benefits could come from the ability to predict earthquakes, volcanic eruptions, and other consequences of either sudden or long-term crustal movement. Repeated geodetic leveling over a significant period of time with adequate connections to tidal stations is one of several measurement techniques that can help solve such problems.

Apparent changes in elevation in an earthquake zone are of special interest. A rough analogy with the stress-strain measurements in the mechanics of materials seems appropriate. A homogeneous elastic material is

Table 1. --Best radius (km) of n point mass anomalies for a sphere with a radius of 6371 km (global case)

n	Best r (km)	n	Best r (km)	n	Best r (km)
10	3603.40	175	5628.46	340	5830.21
15	4070.61	180	5638.31	345	5833.99
20	4350.64	185	5647.78	350	5837.69
25	4544.22	190	5656.86	355	5841.29
30	4688.90	195	5665.62	360	5844.84
35	4802.63	200	5674.06	365	5848.32
40	4895.21	205	5682.20	370	5851.73
45	4972.54	210	5690.05	375	5855.08
50	5038.48	215	5697.64	380	5858.36
55	5095.60	220	5704.97	385	5861.57
60	5145.73	225	5712.07	390	5864.73
65	5190.20	230	5718.94	395	5867.83
70	5230.00	235	5725.59	400	5870.87
75	5265.93	240	5732.05	405	5873.85
80	5298.57	245	5738.30	410	5876.79
85	5328.40	250	5744.38	415	5879.67
90	5355.81	255	5750.28	420	5882.49
95	5381.11	260	5756.00	425	5885.27
100	5404.54	265	5761.57	430	5888.01
105	5426.36	270	5767.00	435	5890.69
110	5446.73	275	5772.28	440	5893.34
115	5465.81	280	5777.42	445	5895.93
120	5483.72	285	5782.43	450	5898.49
125	5500.59	290	5787.31	455	5901.00
130	5516.51	295	5792.08	460	5903.48
135	5531.54	300	5796.72	465	5905.91
140	5545.82	305	5801.26	470	5908.31
145	5559.37	310	5805.68	475	5910.67
150	5572.26	315	5810.00	480	5912.97
155	5584.54	320	5814.23	485	5915.26
160	5596.26	325	5818.36	490	5917.52
165	5607.47	330	5822.39	495	5919.74
170	5618.19	335	5826.34	500	5921.92

said to obey Hooke's law. If stress is increased at a uniform rate, deformation of a test specimen also increases at a uniform rate up to the yield point. A nonlinear response to increased stress at a uniform rate indicates the yield point. In a sense, failure of the specimen has already occurred even though the impending rupture is slightly delayed. Detection of the yield point before rupture actually occurs is tantamount to predicting that an actual rupture will occur. Because of nonhomogeneity and many other causes, the Earth's behavior is by no means as simple as this analogy. Also, the "state of the art" and the availability of long-term repeated geodetic leveling of sufficient precision practically limits crustal movement prediction to linear models at this time. This situation is expected to improve as more leveling data are collected in areas of particular interest. Special consideration of the data needs for crustal movement studies as well as consideration of the traditional geodetic control and engineering uses of height information will improve data density and distribution characteristics. Also, the evolution of analysis methods to a more sophisticated level can be expected to improve the situation in the long run.

This technical report is concerned with the development of a linear prediction model based on point mass anomalies. Such an approach may be productive because it can be logically assumed that crustal movements are accompanied by, if not caused by, some internal mass redistribution within the Earth.

The contemporary strategies and models for predicting vertical crustal movement, based on repeated geodetic leveling in the United States and Canada, were presented in a review paper by Holdahl (1975). Holdahl (1977) has also prepared an up-to-date report on the method preferred and employed by the NOS/NGS (as applied to the "Palmdale Bulge" in southern California). The MQ equation and point mass anomaly approach, as proposed in this presentation, is a variation of that method. Therefore, only that method will be described here, and only to the extent necessary to show the MQ relationship.

COMBINED LEAST-SQUARES ADJUSTMENT AND LEAST-SQUARES PREDICTION

The NGS method associated with vertical crustal movement studies is a combined adjustment and prediction method. A least-squares adjustment of leveling circuits is performed simultaneously with a least-squares prediction of the linear coefficients in a function used to model surface velocities.

Observation equations are developed in the following form (Holdahl 1977):

$$R_{b-a,\ i} = h_{b,\ i} - h_{a,\ i} - \Delta h_{b-a,\ i}. \tag{30}$$

The left hand side is the correction (residual) for an observed height difference between A and B at time t_i. The observed height difference is symbolized with the term $\Delta h_{b-a,\ i}$. The parameters are symbolized with $h_{a,\ i}$ and $h_{b,\ i}$, i.e., the adjusted heights for A and B, also at time t_i. When crustal movement is not a consideration (static Earth model) this formation of observation equations is well known and routine because time t_i is irrelevant. Repeated levelings at different times are an essential ingredient of vertical crustal movement studies; the formulation in eq. (30) is suitable for an expansion to include leveling data of this type.

Conceptually, the height of A at time t_i is the height of A at an earlier time t_o plus the product of the time difference and a constant velocity. Because the surface velocity is variable as a function of position in a study area, it may be expressed as a function of plane coordinates X and Y. For a single bench mark at A, we then have the following expression:

$$h_{a,\ i} = h_{a,\ o} + (t_i - t_o)\ V(X_a,\ y_a). \tag{31}$$

Substituting eq. (31) and a similar one developed for $h_{b,\,i}$ into eq. (30) results in a new observation equation. It has the form:

$$R_{b-a,\,i} = h_{b,\,o} + (t_i - t_o)\, V(X_b, Y_b) - h_{a,\,o} - (t_i - t_o)\, V(X_a, Y_a) - \Delta h_{b-a,\,i}. \tag{32}$$

For this particular case, the new parameters, i.e., the adjusted heights $h_{b,\,o}$ and $h_{a,\,o}$ at time t_o, and the unknown velocities $V(X_b, Y_b)$ and $V(X_a, Y_a)$ have replaced the parameters $h_{b,\,i}$ and $h_{a,\,i}$ in eq. (3). With sufficient redundancy in a set of observation equations, these parameters can be directly solved. However, we will only get discrete velocities at the adjusted circuit junctions where leveling has been accomplished two or more times. An important point should be made here to clarify the adjustment-prediction distinction as previously stated. Generally, there is no provision for incorporating velocity observations directly in eq. (32); $V(X_a, Y_a)$ and $V(X_b, Y_b)$ are unknowns for which observations are not available; only height observations are directly available. An exceptional case occurs if either A or B is a tide gage or Very Long Baseline Interferometry (VLBI) station; otherwise velocity is only an indirect geometric and physical consequence of a height change with elapsed time. Consequently, the heights are "adjusted" by least-squares as a function of direct height difference observations and time differences, whereas the velocities are generally an indirect or "predicted" consequence of the same adjusted observations of height and time differences. It is also desirable to "predict" or interpolate velocities at points away from adjusted circuit junctions. This can be accomplished with continuous "least-squares prediction," which is generally concerned with converting discrete samples of a real continuous function into a reasonable and logical substitute continuous function; hopefully, the substituted function bears a close resemblance to the original unknown function in most of its unmeasured regions. A prediction function previously used in the NGS method has been an ordinary two-dimensional polynomial of the form

$$V(X_a, Y_a) = c_o + c_1 X_a + c_2 Y_a + c_3 X_a Y_a + c_4 X_a^2 + \ldots \tag{33}$$

When this prediction form and its counterpart for $V(X_b, Y_b)$ are substituted in eq. (32), we have the final form for a unit-weighted observation equation involving both least-squares adjustment and least-squares prediction:

$$R_{b-a,\,i} = h_{b,\,o} + (t_i - t_o)\left(c_o + c_1X_b + c_2Y_b + c_3X_bY_b + c_4X_b^2 + \ldots\right) - h_{a,\,o} - (t_i - t_o)\left(c_o + c_1X_a + c_2Y_a + c_3X_aY_a + c_4X_a^2 + \ldots\right) - \Delta h_{b-a,\,i}. \quad (34)$$

In this form, $h_{b,\,o}$ and $h_{a,\,o}$ are the unknown heights at A and B at time t_o. The other unknowns are the polynomial coefficients $c_o, c_1, c_2 \ldots c_n$. The question has arisen as to whether more polynomial coefficients can be determined in eq. (34) than the number of unknown but determinable velocities in eq. (32). The indications are negative, which seems reasonable based on the combined least-squares adjustment/least-squares prediction nature of the solution and some of the known limitations of each procedure by itself. This is part of a solvability problem that has been discussed in another paper (Holdahl and Hardy 1977).

After the unknowns are determined from observation equations of the type given in eq. (33), it is easy to recover any height at any time t_i by a set of equations similar to that in eq. (31). Moreover, a continuous prediction of the surface velocities in the study region can be accomplished by evaluating and contouring a discrete set of evaluated $\tilde{V}_p$'s in the form

$$\tilde{V}(X_p, Y_p) = c_o + c_1X_p + c_2Y_p + c_3X_pY_p + c_4X_p^2 + \ldots \quad (35)$$

Many surface fitting techniques could be used to replace the ordinary polynomial series in eq. (33). The apparently advantageous properties of MQ equations in many applications as reported by the author and others have led to

considering the MQ method in this report. The modification is very simple. We let

$$V(X_i, Y_i) = \sum_{j=1}^{n} \omega_j Q(X_i, Y_i, X_j, Y_j) \quad i = 1, 2 \ldots m \quad m \bar{>} n \tag{36}$$

in which the $V(X_i, Y_i)$'s, i = 1, 2, 3, ..., correspond to $V(X_a, Y_a)$, $V(X_b, Y_b)$, $V(X_c, Y_c)$,,,. and the X_j, Y_j's are nodal points with their associated coefficients ω_j. These equations can be substituted in eq. (32) and will produce an observation equation similar to that in eq. (34) in which the MQ coefficients are unknowns instead of the polynomial coefficients. After a least-squares solution, the predicted velocities are determined by using the determined coefficients ω_j in the form

$$\tilde{V}(X_p, Y_p) = \sum_{j=1}^{n} \omega_j Q(X_p, Y_p, X_j, Y_j). \tag{37}$$

There is no change in the method of determining adjusted heights at any time t_i.

PHYSICAL INTERPRETATION OF THE MULTIQUADRIC COEFFICIENTS

If the quadric kernel in eq. (36) is a reciprocal hyperboloid, a physical relationship to point mass anomalies is involved in some way in accordance with the previous discussion concerning eq. (3). Collectively, the MQ prediction of a single velocity at X_p, Y_p, as in eq. (37), is the sum of contributions from n kernel functions, each of which is a reciprocal distance times a numerical coefficient. Because the end result is the velocity $\tilde{V}(X_p, Y_p)$, each contribution must be regarded as a linear component of that velocity. All surface velocities V(X, Y) are clearly the rate that topographic heights change with time, i.e., $\partial H/\partial t$. The height H is also a function of X and Y. This is reflected in eq. (5) involving the hyperboloid as an MQ kernel.

Note that we purposely used ω_j's as coefficients in eqs. (36) and (37) instead of α_j's as in eqs. (4) and (5). Although the ω_j's are related to the α_j's, it should not be expected that they have exactly the same interpretation because the crustal movement problem involves velocities. Let us postulate that

$$\omega_j = \frac{\partial \alpha_j}{\partial t} = \text{constant}$$

i.e., that the ω_j's represent the constant rate that the point mass anomalies α_j are changing with time. This is certainly consistent with eq. (4) in which we can partially differentiate disturbing potential T with respect to time t. Substituting ℓ_j^{-1} for the quadric kernel and partially differentiating, the result is

$$G \sum_{j=1}^{n} \alpha_j \left(\frac{\partial \ell_j^{-1}}{\partial t} + \ell_j^{-1} \frac{\partial \alpha_j}{\partial t} \right) = \frac{\partial T}{\partial t} \, . \tag{38}$$

In eq. (4), the quantity T is a continuous physical variable, and the α_j's may be regarded as discrete samples of a continuous physical variable. The ℓ_j^{-1}s are fundamental geometric quantities only. If we try to evaluate the differential eq. in (38) to find any particular $(\partial T/\partial t)_i$, we find that we must specify a series of ℓ_{ij}^{-1}'s. These are the fixed reciprocals of distances connecting a point of prediction, on a plane, to n discrete and fixed points with coordinates (X_j, Y_j, δ) which represent the location of point mass anomalies. In Euclidean geometry, there is no rate of change of the geometry itself with time. Consequently, $\partial \ell_j^{-1}/\partial t_j = 0$. Thus, eq. (38) reduces to

$$G \sum_{j=1}^{n} \frac{\partial \alpha_j}{\partial t} \ell_j^{-1} = \frac{\partial T}{\partial t} \, . \tag{39}$$

This functionally relates a change in a point mass anomaly with time to a change in the disturbing potential with time.

A similar approach with eq. (5) leads to

$$\frac{G}{K} \sum_{j=1}^{n} \frac{\partial \alpha_j}{\partial t} \ell_j = \frac{\partial H}{\partial t} , \tag{40}$$

which together with eq. (39) implies a consistent theoretical point mass anomaly relationship between changes in height H with time and changes in some equivalent form of disturbing potential T with time. What is not expressed in eqs. (39) and (40) at this time are the scale factors and other refinements associated with the factor K that would reduce the given geometric and dynamic relationships to point mass anomaly models that are theoretically equivalent; a first attempt at a scale reconciliation is given near the end of this report. Hardy (1976) has shown that gravity anomalies can be predicted equally well in Cartesian coordinates with MQ formulations based on either eqs. (4) or (5), although the theoretical basis has not been completely established.

In making this study, it was suspected that similar results would be found when applied to crustal movement studies. The following sections confirm this anticipated result.

THE ERROR OF PURE PREDICTION

For this study, we isolated the pure prediction properties of a prediction function from the associated computational procedures in practice which sometimes confuse the development of a new method. The concept involves using a continuous "error-free" model, "error-free" data samples, and developing a unique solution, which causes the "prediction" function to fit the continuous, "error-free" function exactly at all sample points. This is related to the collocation polynomial approach (Scheid 1968, Hardy 1971) which should not be confused with "collocation" as frequently used in geodesy by Moritz (1972) and others. As will be seen later, the objective of this approach is to judge the performance of a prediction function by comparing predicted ordinates with the "error-free" ordinates at the same locations for a particular number of prediction points. In other words, for the purposes of this study we define

"pure prediction" as a critical confrontation and comparison of predicted values with true values of a realistic error-free function, away from data points that are fitted exactly.

The standard error of least-squares prediction for covariance functions, as given by Heiskenan and Moritz (1967, p. 269) does not, in fact, compare predicted values with the corresponding true values. Instead, it estimates the error of the random stochastic model in fitting the sample points (Kearsly 1977)--something quite different than the error of pure prediction as used in this study.

In figure 1, we see a contoured plot of subsidence (in feet) in the Houston-Galveston area for 1942 to 1973. This was used, as will be seen later, as the basis for a fictitious, but realistic contour plot of surface velocities in cm/yr for the same area.

Figure 2 shows a rectangular grid pattern to cover the study area, used for two purposes:

(1) It defined the location of 49 grid intersections that would be the discrete prediction points for all prediction functions used in the test.

(2) It provided the basis for a simulation of data collection in the study area. One sample location was chosen at random in each of 36 grid rectangles. Thirteen additional sample locations were chosen within the boundary of the study area in an "at large" manner, thus providing 49 irregularly spaced sample points.

Figure 3 shows the continuous "error-free" model drawn by Holdahl, independently of the grid intersection and random sample locations. Figure 4 shows an overlay of the sample locations on the "error-free" model. The sample points completely missed several important subsidence features and sections of contour lines, which possibly would not have happened if the "error-free" function had been "visible" or known a priori. Figure 5 shows these features and partial contour lines. The missing features illustrate an

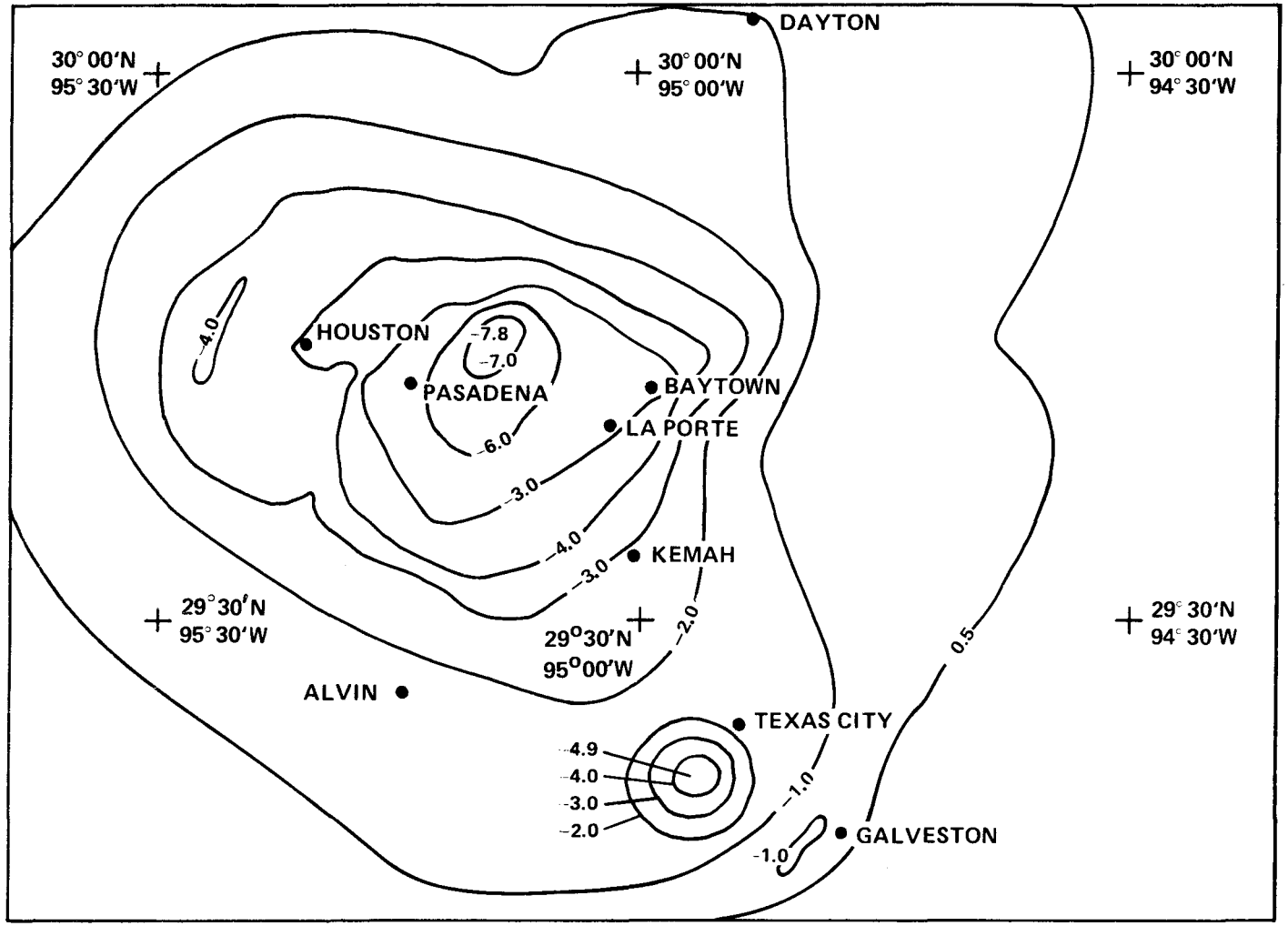

Figure 1.--Original map of Houston-Galveston Subsidence Area (1942-1973); contours of subsidence are given in feet (1 ft = 0.3048 m).

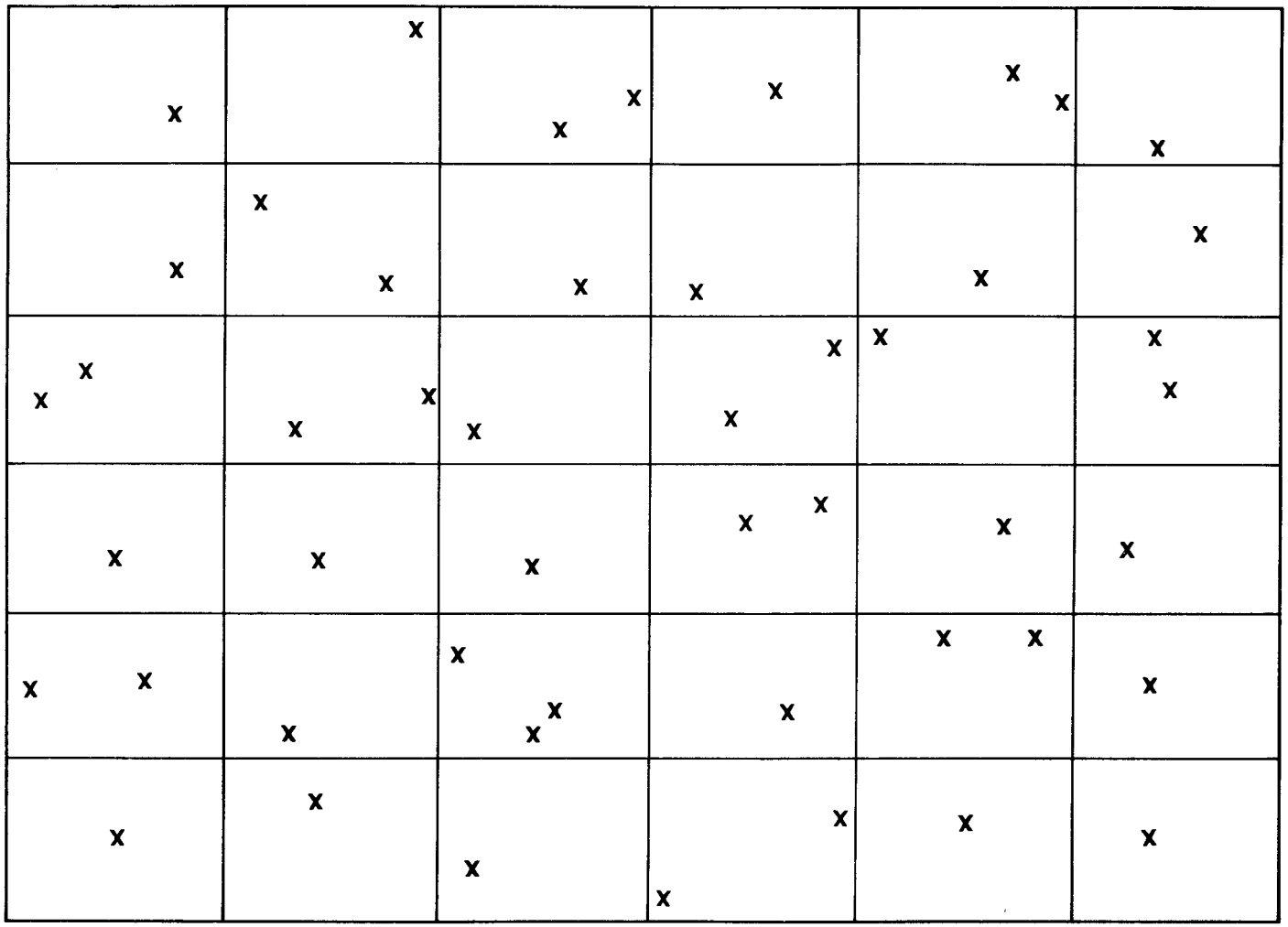

Figure 2.--Rectangular grid over the Houston-Galveston subsidence area with sample point locations.

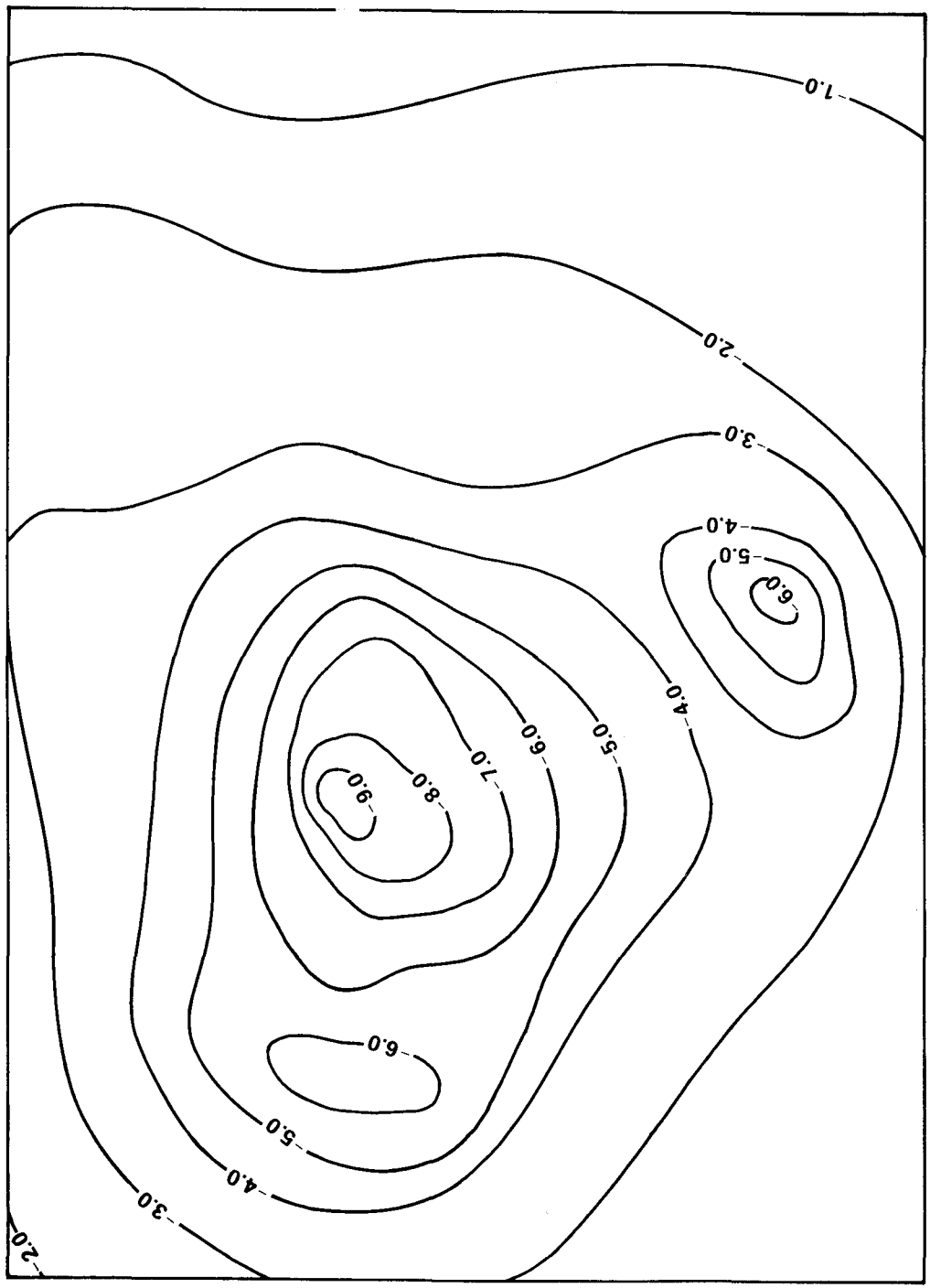

Figure 3.--Error-free surface velocity model (cm/yr).

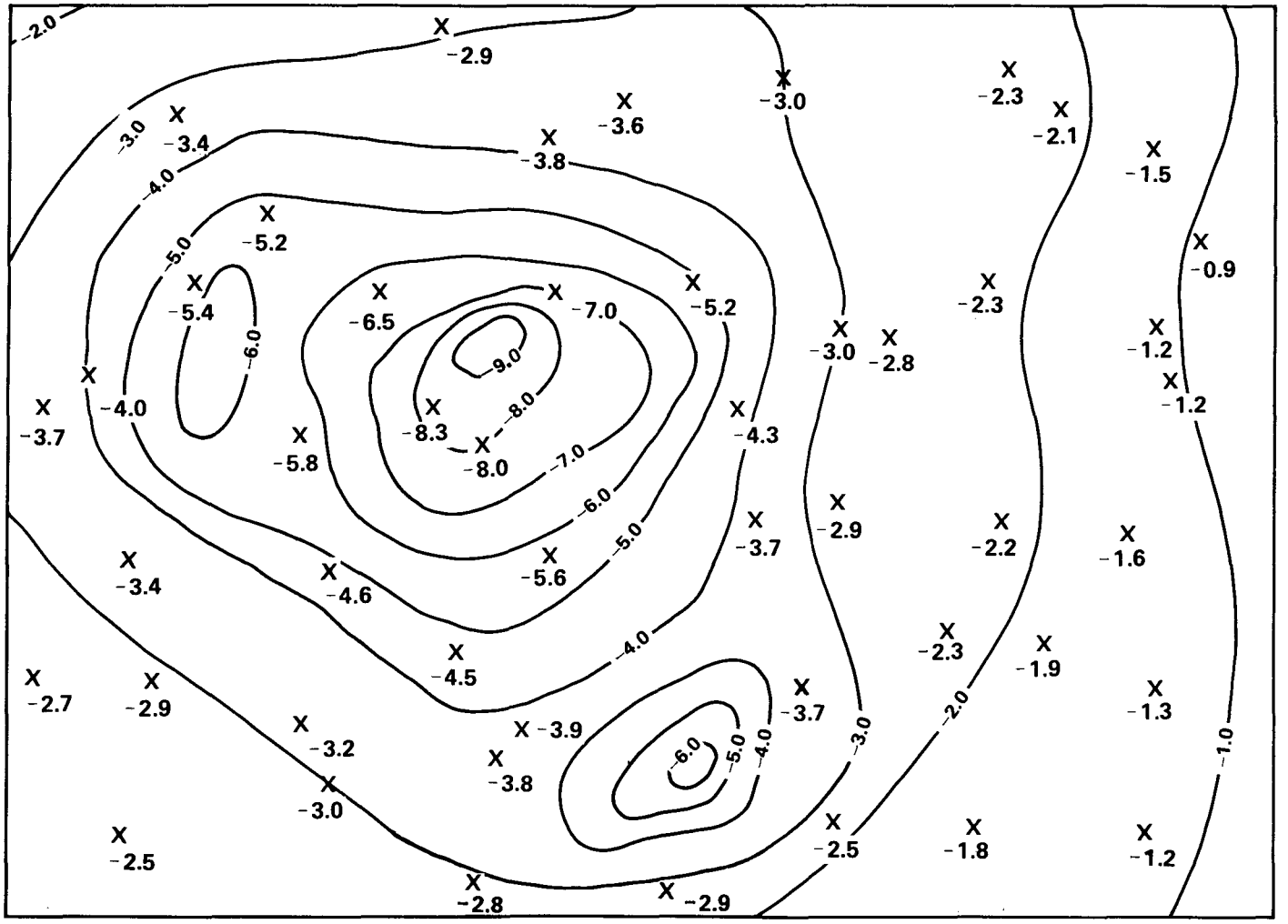

Figure 4.--Overlay of sample point locations and ordinate values (cm/yr) on the "error-free" surface velocity model.

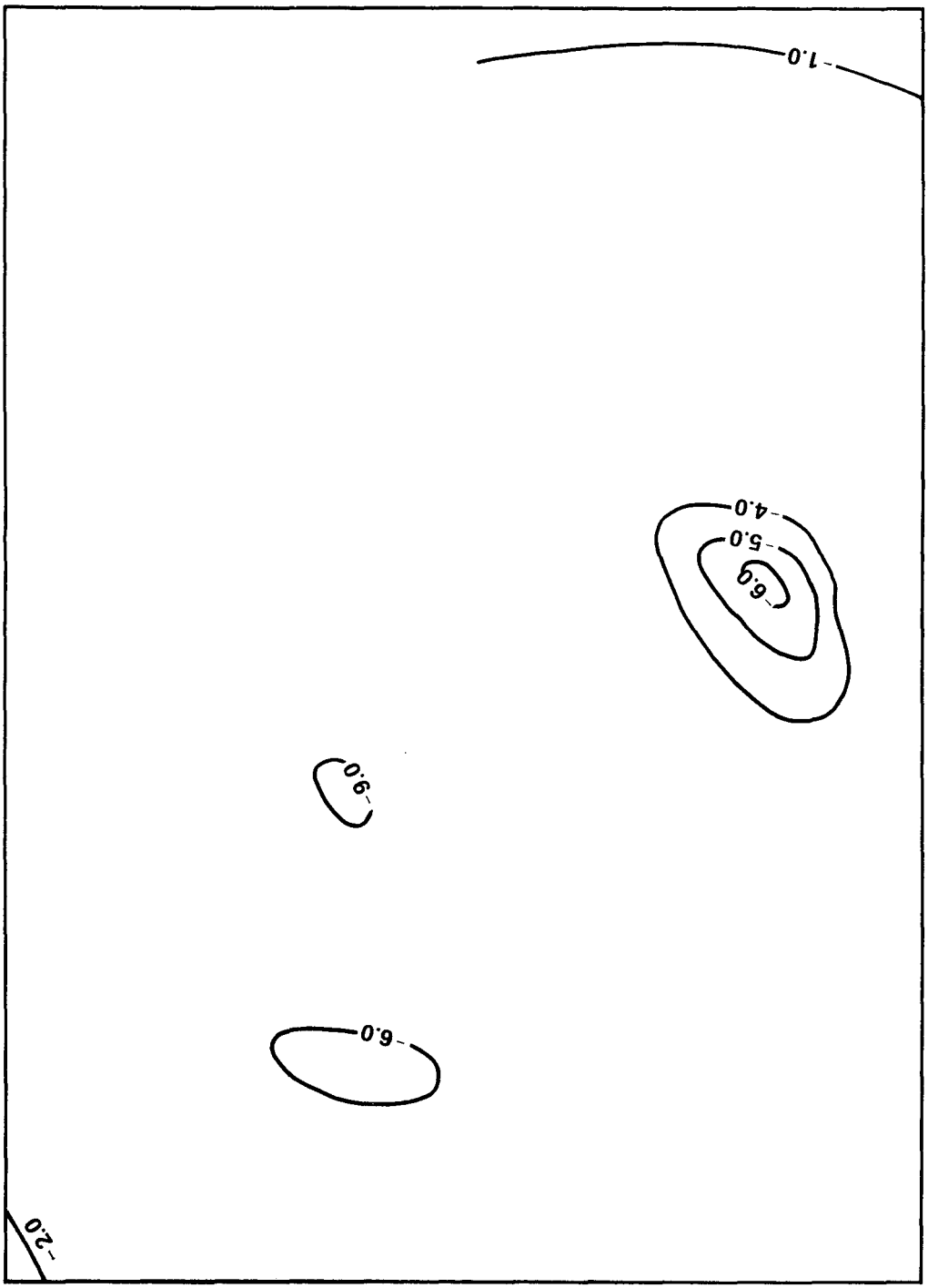

Figure 5.--Features and contour sections (cm/yr) missed by the sample point locations.

important point in using apparent or empirical covariance functions as a basis for prediction. It is obvious that the missed features of the continuous "error-free" function significantly contribute to the true variance of the "error-free" function. Consequently, the true variance of a real phenomenon is generally larger than that determined from the sample variance. When an empirical covariance function is normalized to unity for the variance, the division is usually done with a number that is too small. Unfortunately, there seems to be no way of predicting in advance how small this number will be. The contemporary result of the normalization is to produce an apparent covariance function that is too large at small distances. This phenomenon also affects the computation of degree variances that may be substituted into what are otherwise deterministic functions. This discussion of defects in apparent covariance is not meant to imply that MQ or any other deterministic prediction method will miraculously predict features that have not been sampled. On the other hand, MQ functions of the deterministic kind are not handicapped by this described defect in the apparent covariance, or degree variances based on sampling, because covariances in a statistical sense are not used as the basic function.

We will now complete the discussion of pure prediction, and describe the accomplishment of the comparative tests. Figure 6 shows an overlay of the prediction grid intersections on the "error-free" model. Prediction points are located in two of the three major features missed by the data samples. The spot velocities indicated in figures 4 and 6 were carefully interpolated for the 49 sample points and 49 predicted points respectively. Although the interpolations could be disputed from the present view of being "error free," this would pointlessly require a redefinition of pure prediction as previously defined. The model is a logical surface velocity model associated with the Houston-Galveston subsidence area. The interpolations are logical, if not explicitly perfect. The philosophy of this type of test dictates that "the model could be error free; therefore, it is." In other words, the assumed "error-free" prediction points and assumed "error-free" sample points define the discrete "error-free" model. The contours themselves may be viewed as an inaccurate graphical representation of the "error-free" model, symbolizing continuity. Consequently, the "error-free" model thus defined provides a

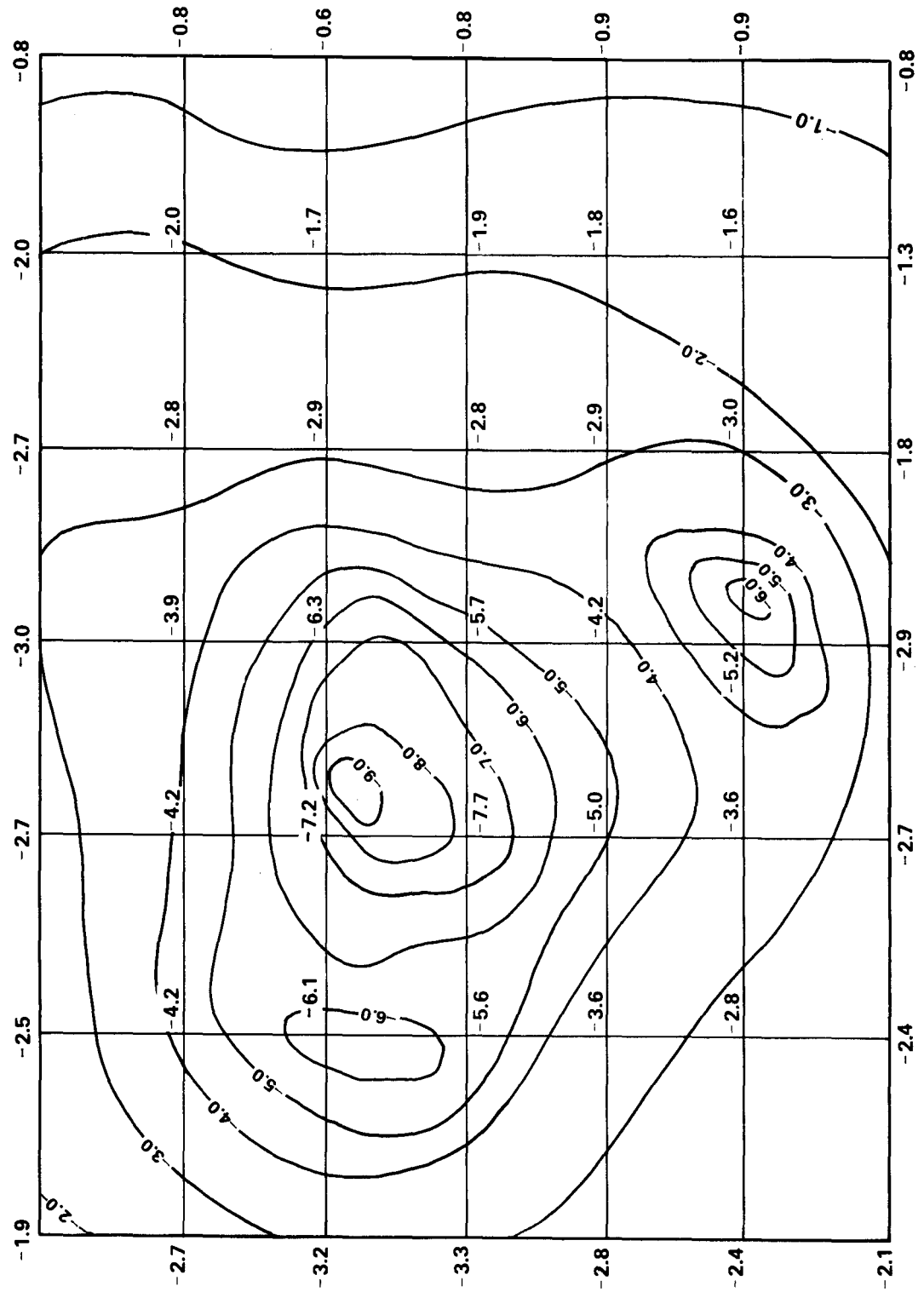

Figure 6.--Overlay of grid prediction points (cm/yr) on the error free model.

beginning point for comparing prediction functions on an equitable basis. It is assumed that the subsequent refinement by least-squares or other filtering and smoothing techniques, presumably unbiased, will not adversely affect the pure prediction capability of the function. In any case, all functions make use of the same data, and are required to make predictions of the same points. The quality of the prediction methods are judged relatively by their capability to replicate the "error-free" model at a particular number of prediction points. All useful prediction methods will presumably approach the continuous error-free model arbitrarily close with sufficient data points, in accordance with the Weierstrass theorem. What is being tested, however, is not the basic logic of the prediction method, but the pure accuracy. Other considerations being equal, the efficiency is an indirect, but important, consideration because a more accurate method can presumably equal the performance of less accurate methods by using fewer sample points.

COMPARATIVE RESULTS OF THE PURE PREDICTION TEST

The following prediction functions were used for comparative tests of the "error-free" model (fig. 3):

- MQ forms (n = 49)

  Conic kernel:

$$\frac{G}{K} \sum_{j=1}^{n} \omega_j \left[\left(X - X_j \right)^2 + \left(Y - Y_j \right)^2 \right]^{1/2} = V(X,Y). \tag{41}$$

  Hyperboloid kernel:

$$\frac{G}{K} \sum_{j=1}^{n} \omega_j \left[\left(X - X_j \right)^2 + \left(Y - Y_j \right)^2 + \delta^2 \right]^{1/2} = V(X, Y) \tag{42}$$

  a) δ = 5.62 km

  b) δ = 12.51 km

  c) δ = 14.19 km

  d) δ = 15.90 km

Reciprocal hyperboloid kernel:

$$G \sum_{j=1}^{n} \omega_j \left[\left(X - X_j\right)^2 + \left(Y - Y_j\right)^2 + \delta^2 \right]^{-1/2} = V(X, Y) \qquad (43)$$

a) δ = 3.98 km

b) δ = 5.62 km

c) δ = 7.62 km

d) δ = 9.74 km

- Bi-sixth degree polynomial (49 terms)

Form:

$$\sum_{i=o}^{6} \sum_{j=o}^{6} c_{ij} X^i Y^j = V(X, Y). \qquad (44)$$

The last function is not an MQ equation, but was included for comparison because it is a typical polynomial form previously used in crustal movement studies. It does not have a geophysical interpretation related to point mass anomalies, and is called a bi-sixth degree polynomial because it is formed in a manner similar to the well known bi-cubic polynomial.

Figures 7 through figure 15 show graphical representations of the continuous surface velocity predictions for each of the MQ functions above. The contours for each function were interpolated with respect to velocities at 49 irregularly spaced data points that were fitted exactly by the interpolation function (except for minor roundoff errors), plus the predicted velocities of each function at 49 regularly spaced rectangular grid intersections.

Table 2 gives the statistical results for the MQ functions. The bi-sixth degree polynomial was fitted exactly to data points, but gave such erratic predictions between data points that neither the contouring nor statistics are presented; this seems to be a common defect of higher degree polynomials.

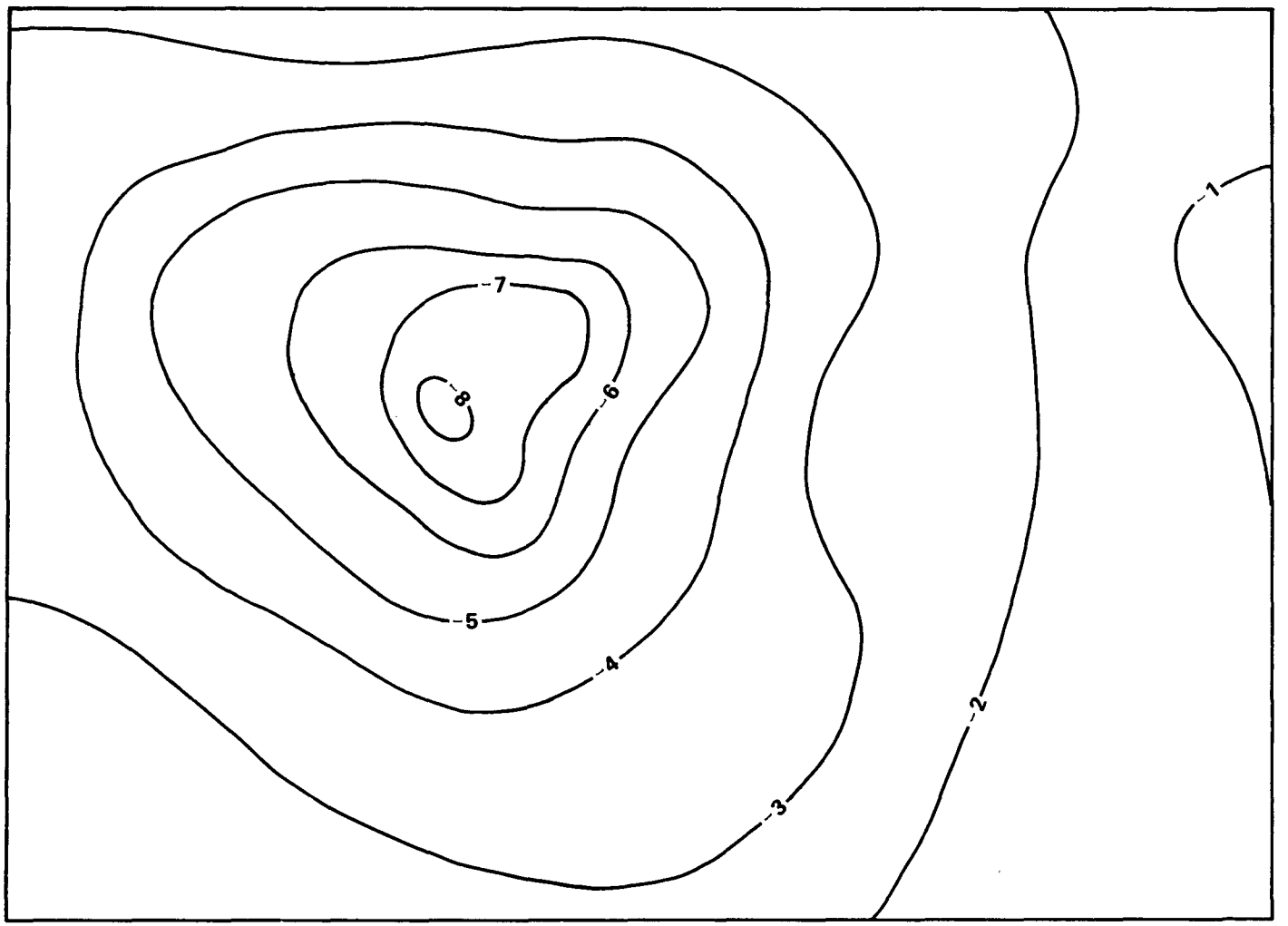

Figure 7.--MQ prediction (cm/yr) with the cone as a kernel, $\delta = 0$.

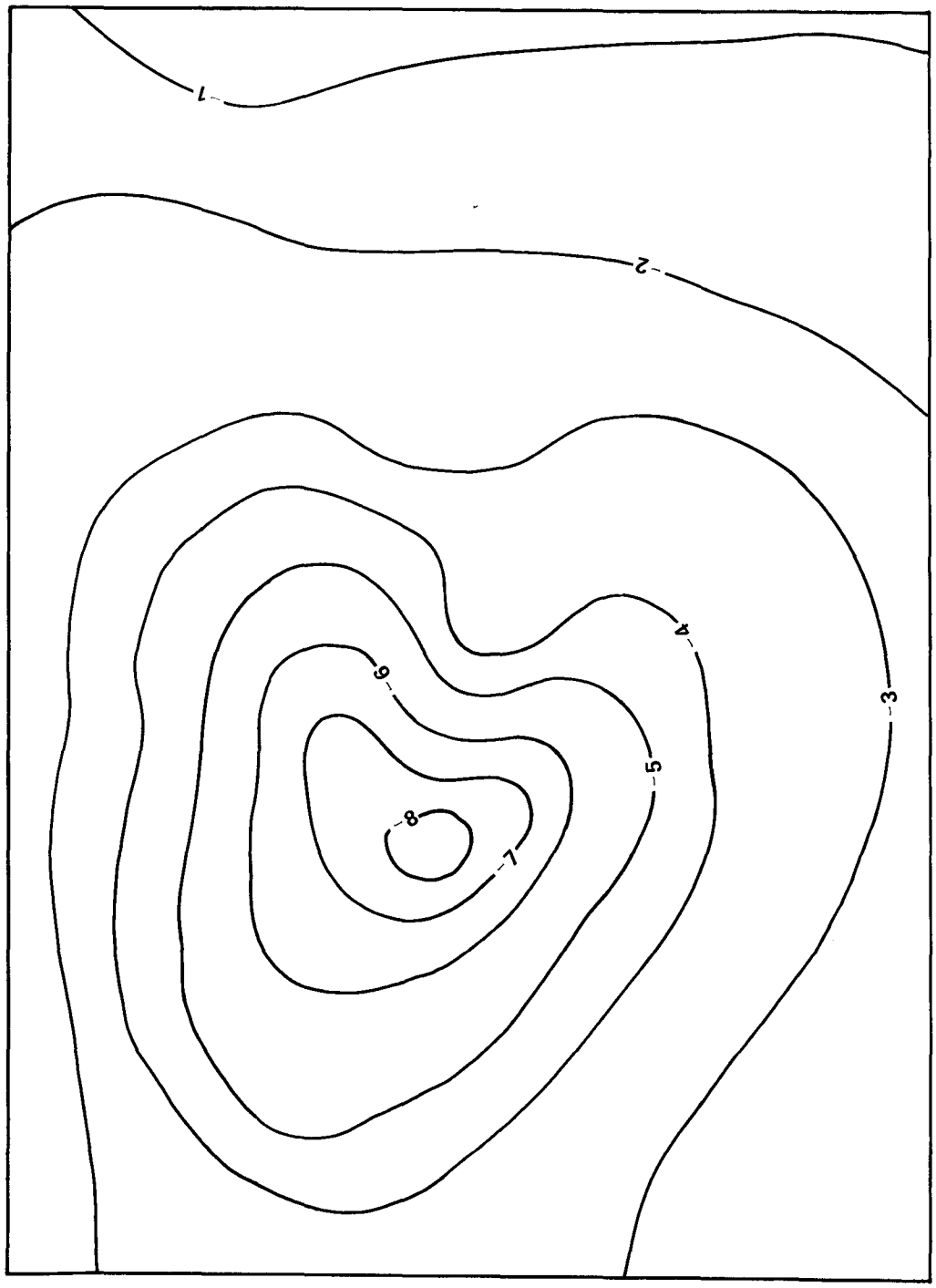

Figure 8.--MQ prediction (cm/yr) with a hyperboloid as the kernel, δ = 5.62 km.

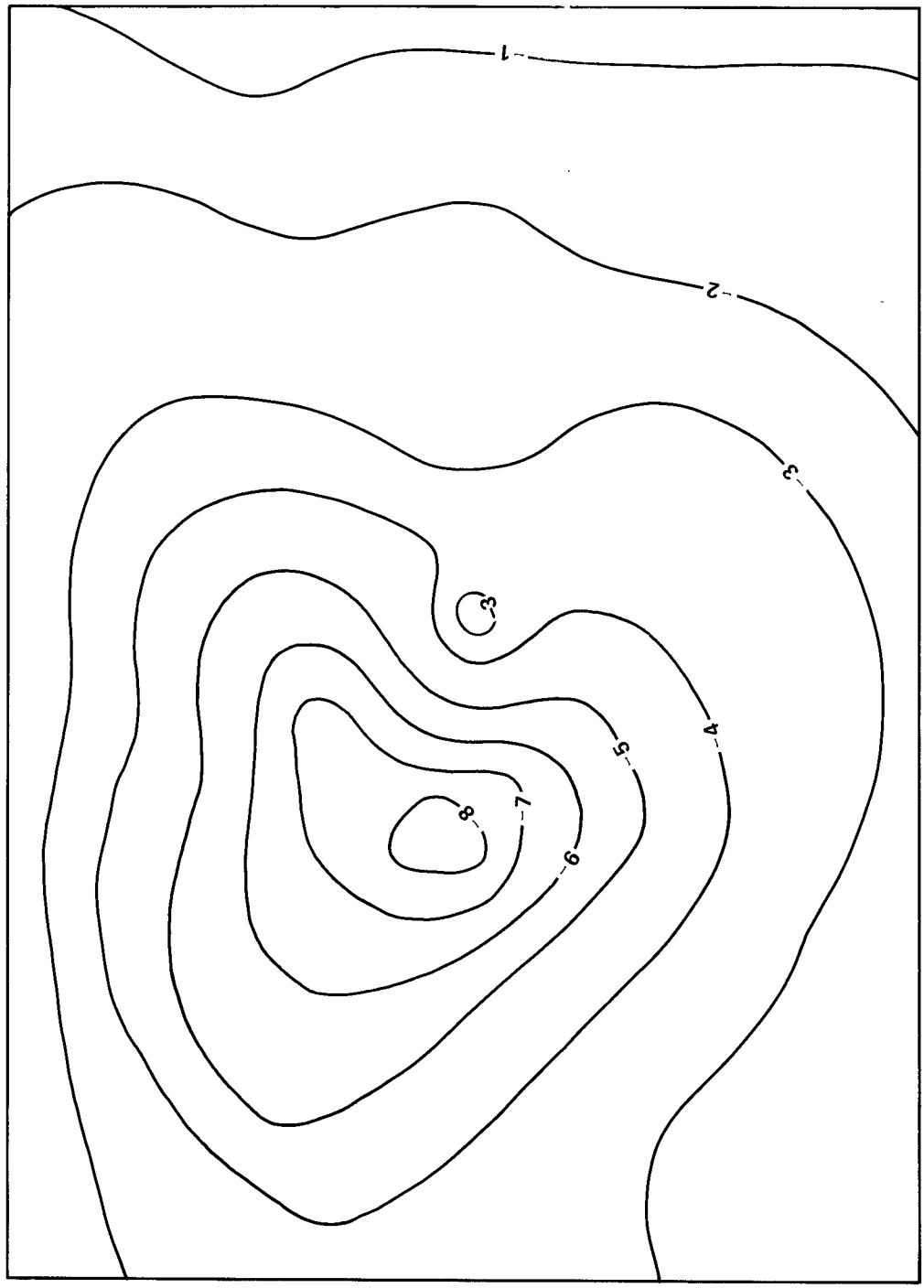

Figure 9.--MQ prediction (cm/yr) with a hyperboloid as the kernel, δ = 12.51 km.

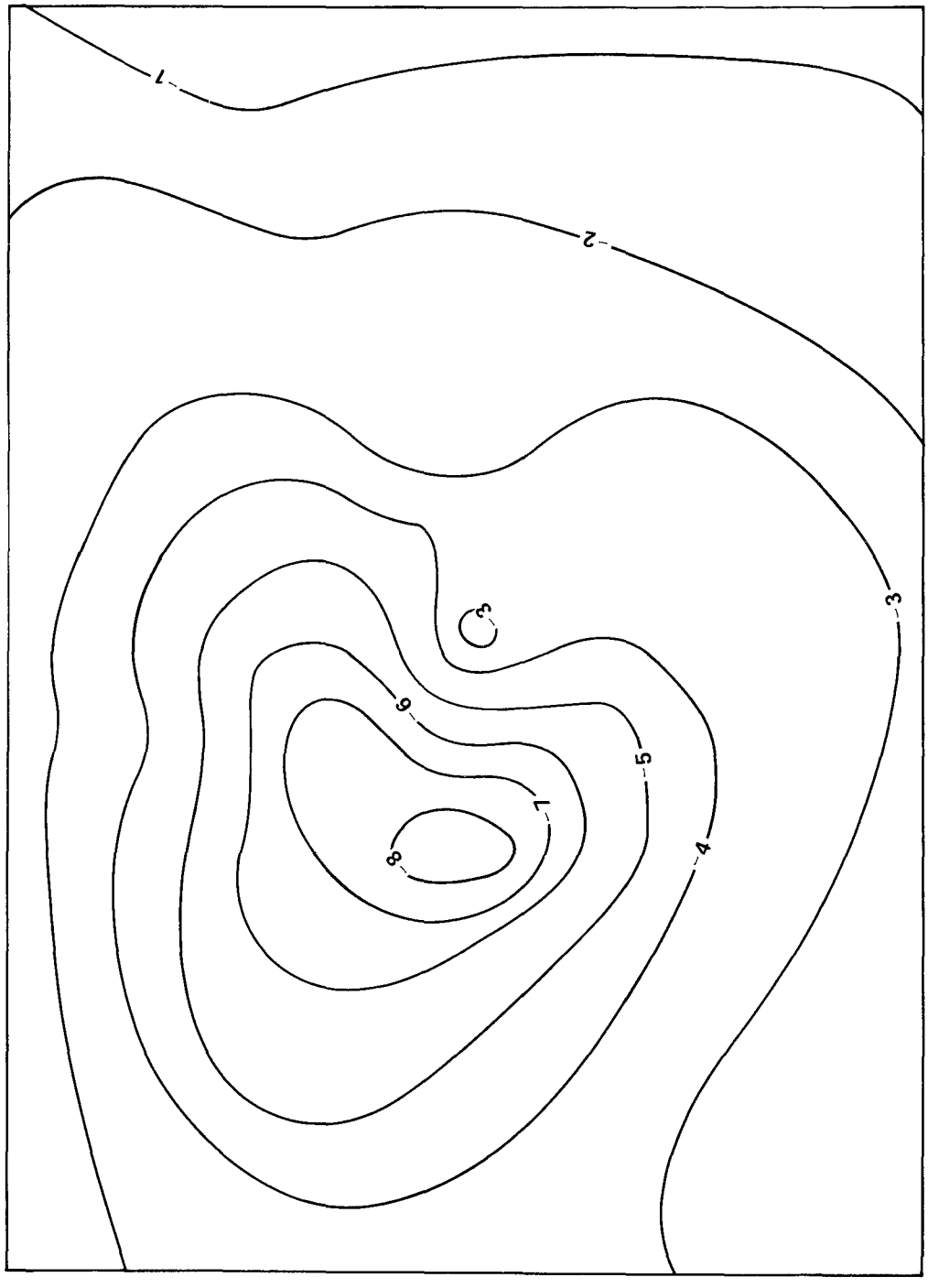

Figure 10.--MQ prediction (cm/yr) with a hyperboloid as the kernel, δ = 14.19 km.

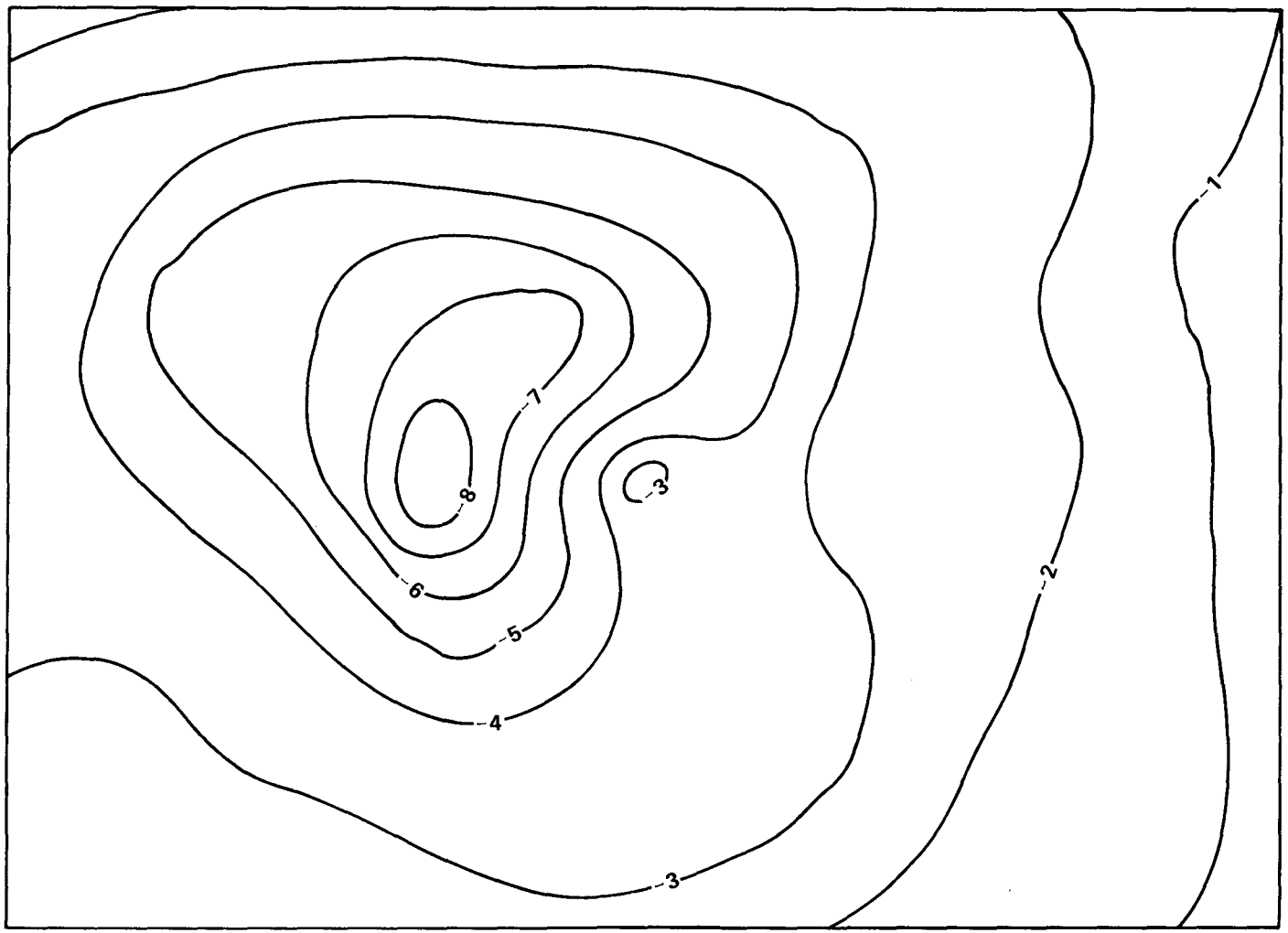

Figure 11.--MQ prediction (cm/yr) with a hyperboloid as the kernel, δ = 15.90 km.

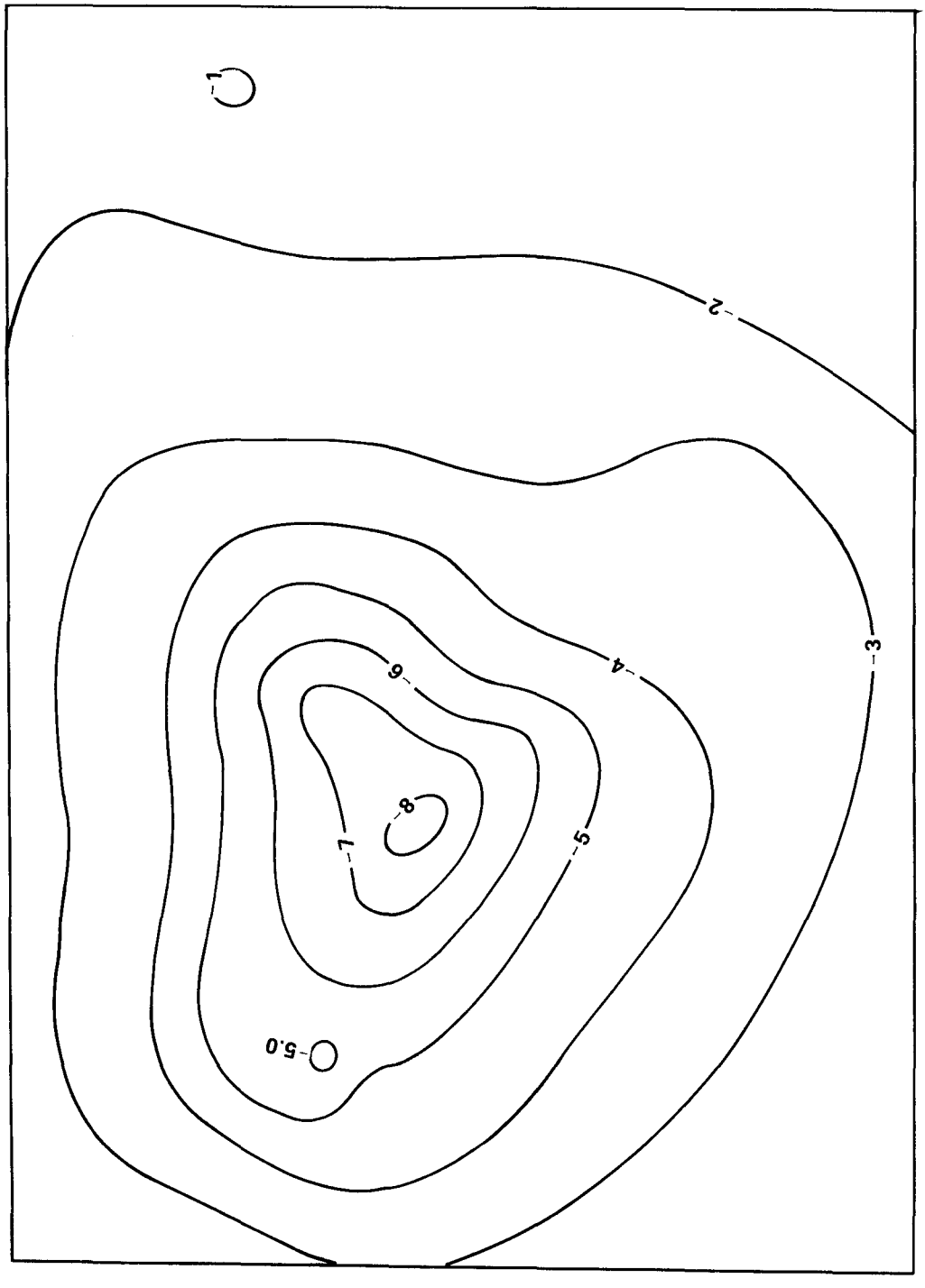

Figure 12.--MQ prediction (cm/yr) with a reciprocal hyperboloid as the kernel, δ = 3.98 km.

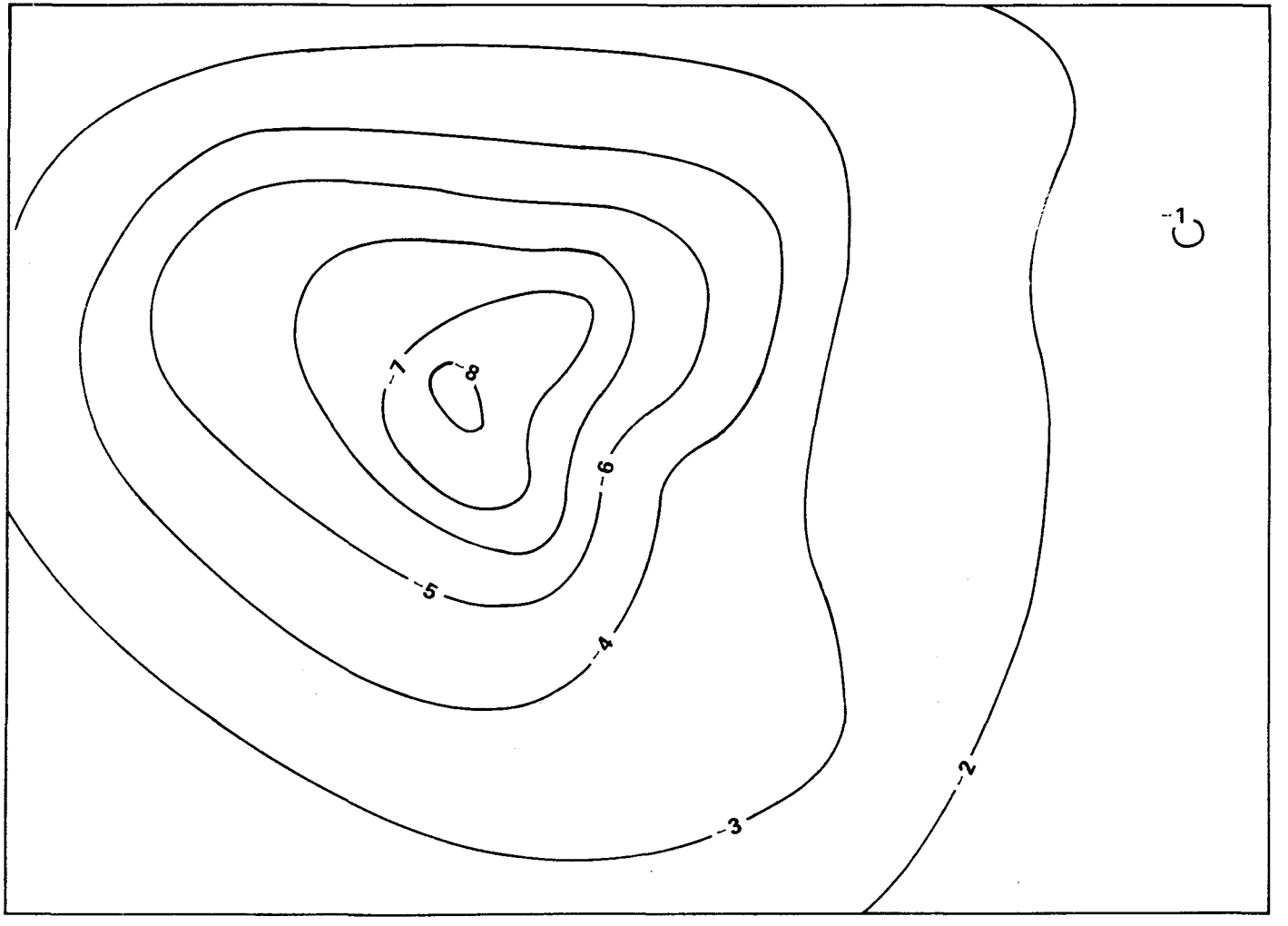

Figure 13.--MQ prediction (cm/yr) with a reciprocal hyperboloid as the kernel, δ = 5.62 km.

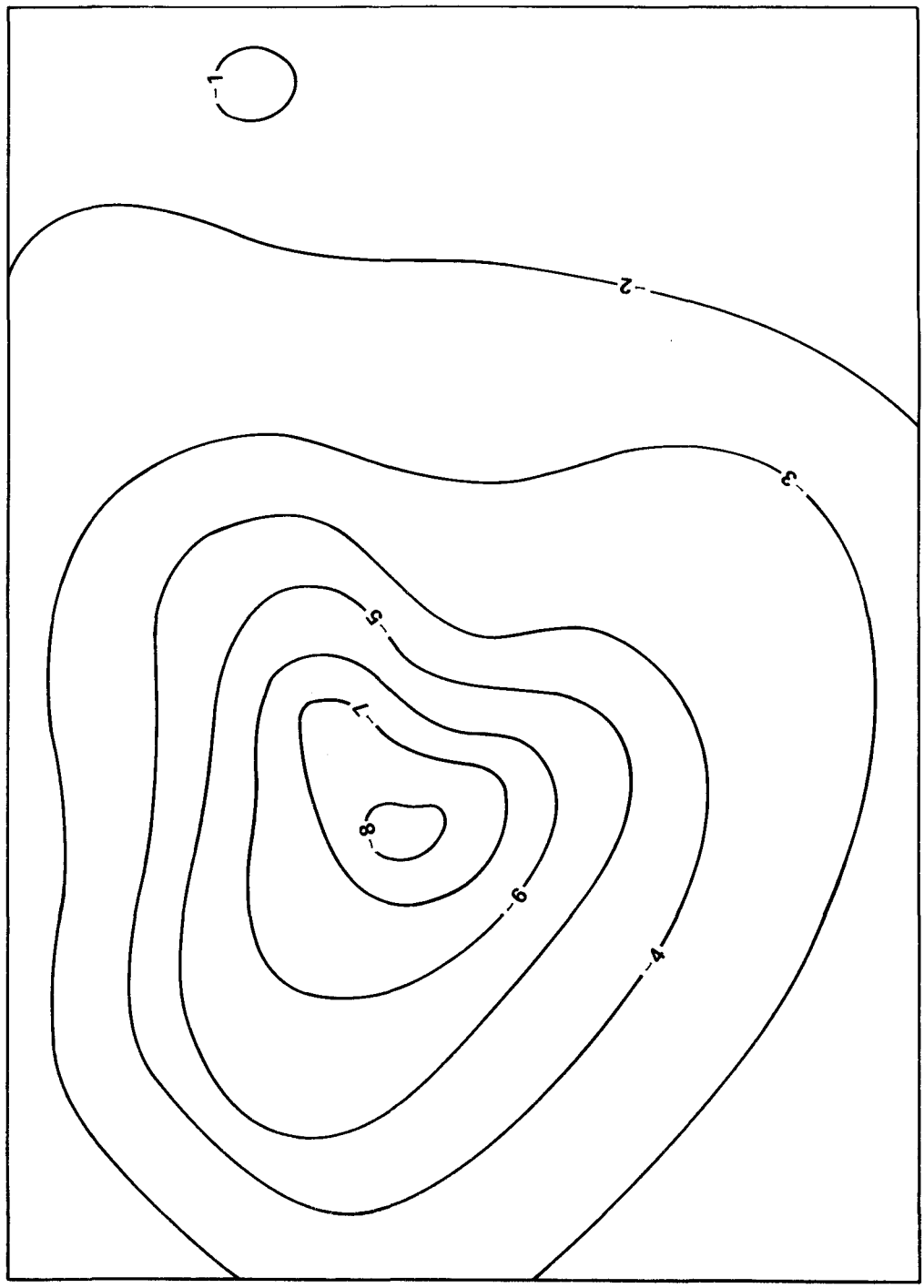

Figure 14.--MQ prediction (cm/yr) with a reciprocal hyperboloid as the kernel, δ = 7.62 km.

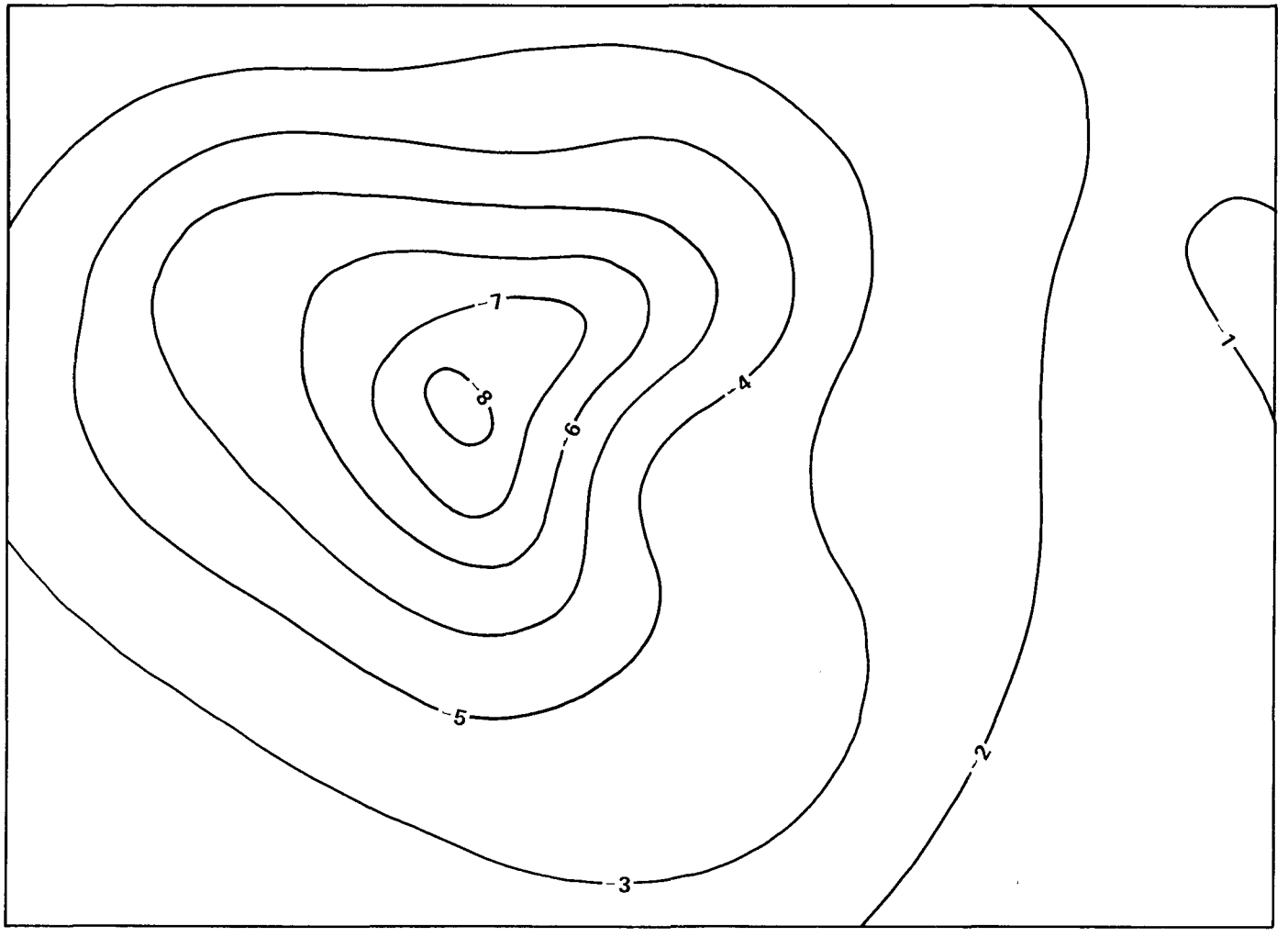

Figure 15.--MQ prediction (cm/yr) with a reciprocal hyperboloid as the kernel, δ = 9.74 km.

Table 2.--Accuracy of surface velocity prediction

Function (δ in km)	Maximum error (cm/yr)	Standard error (σ_s) of a single prediction (cm/yr)
Multiquadric forms		
Conic kernel	+ 1.63	± 0.44
Hyperboloid kernel		
a) δ = 5.62	+ 1.85	± 0.46
b) δ = 12.51	+ 2.83	± 0.60
c) δ = 14.19	+ 3.02	± 0.63
d) δ = 15.90	+ 3.19	± 0.67
Reciprocal hyperboloid kernel		
a) δ = 3.98	+ 2.05	± 0.56
b) δ = 5.62	+ 1.88	± 0.46
c) δ = 7.62	+ 1.77	± 0.43
d) δ = 9.74	+ 1.88	± 0.45
Bi-sixth polynomial	n.a.	n.a.

GEOPHYSICAL INTERPRETATION OF THE RESULTS

From a purely geometric point of view, predictions of the surface velocities in the Houston-Galveston area were done very well by the MQ functions. The contoured results in figures 7 through 15 are remarkably similar, although the depth of point masses δ was varied considerably during the test. Using the statistical results in table 2 as a guide in lieu of the graphical results, the best nonharmonic form and the best harmonic form of the MQ functions performed almost equally well. As indicated above, the bi-sixth degree polynomial did not perform adequately. Consequently, only MQ functions will be discussed in this section of the report.

The best statistical result, i.e., a standard error, σ_s = 0.43 cm/yr, was obtained using a reciprocal hyperboloid kernel with a point mass anomaly at a depth δ of 7.62 km. This depth was estimated a priori to be optimum by

using eq. (28). Thus, the practical use of this formula for "flat Earth models" has been confirmed.

The best statistical result among the nonharmonic MQ forms was obtained with the cone as a kernel. With a standard error, σ_s = 0.44 cm/year, the error estimate is only slightly worse than the best reciprocal hyperboloid. For the conic form, which is a so-called degenerate hyperboloid, $\delta = 0$. Although the surface of an MQ formulation involving cones is continuous, its first derivative is discontinuous at the nodal points. This discontinuity can be removed by assigning an arbitrarily small δ, e.g., $\delta = 1^{-10}$ km, which would have no detectable effect on either the prediction or the σ_s = 0.44 cm/yr.

It should be noted that the standard error of MQ prediction with hyperboloid kernels increased steadily as the depth δ was increased, in contrast with the reciprocal hyperboloid. The depth, δ = 14.19 km, was one of several depths used in the series because it is the result obtained with the a priori use of the empirical formula in eq. (29). This formula was developed a few years ago by a best fit to a bi-cubic spline function. Although the prediction at this depth of mass anomalies does not seem unreasonable (fig. 10), table 2 shows that it is certainly not optimum in this comparison.

In some applications, perhaps a more rigorous development of the point mass anomaly concept, it may be found that an interaction between harmonic and nonharmonic functions requires the use of the same depth δ in both cases. The optimum δ = 7.62 km for the harmonic form was not used with the nonharmonic form in this test. However, an estimate of the standard error, i.e., σ_s = 0.49, can be obtained for the use of a hyperboloid with δ = 7.62 km, by linear interpolation in table 2 between δ = 5.62 km and δ = 12.51 km. In this connection it is interesting, but may be of no special significance, that for δ = 5.62 km, the standard error, σ_s = 0.46, is exactly the same for both the reciprocal and hyperboloid kernels.

A completely rigorous geophysical interpretation of the results of this test cannot be made because of the newness of the concept of using point mass

anomaly models for crustal movement studies. Also, the test area in the Houston-Galveston area involves subsurface changes that are much nearer the topographic surface than the depths of point mass anomaly sets that were optimum for the reciprocal hyperboloid. The average spacing of surface data was about 17.8 km for which the optimum depth is 7.62 km, according to eq. (28). Denser data sets are needed to provide detailed information about mass redistribution at shallow depths.

Subsidence in the Houston-Galveston area is generally attributed to lowering of the water table by excessive use of ground water as a water supply source. In other words, subsidence is the result of removal of a considerable amount of fluid mass and reduction of fluid pressure followed by a compression of de-watered clay layers. Geometrically, the surface has simply been lowered. Physically, the average density of material relatively near the surface has increased. There was probably little or no change in the mass distribution at the 7.62 km depth. Although the coefficients of the point mass anomalies at 7.62 km have changed as the subsidence progressed, they certainly did not change as much as they would have for shallower point mass anomaly sets.

Another important factor has placed limitations on the details of geophysical interpretation that can be accomplished with this first test. The data used for this test consisted only of velocity data for subsidence with respect to the original terrain surface. Details of heights above mean sea level as of 1942 and 1973 were not used, which is of no consequence for fitting the data ordinates of the subsidence velocities in a purely geometric sense. It could affect determining the point mass anomalies, and consequently, the associated interpretation of them. There may have been no correlation between the rates of subsidence with the absolute heights of the topography in the region, but without studying that aspect, one cannot be certain. Obviously, a fit to the subsidence velocities had to be based on a constant height reference plane (equivalent conceptually to mean sea level) in the absence of the detailed topography.

Also, because of the as yet undetermined K factor in the use of the hyperboloid kernel, gravity anomalies are needed. The K factor appears

theoretically related to an isostatic terrain model, but in practice, it must also include some characteristics of a heuristic constant, reflecting the actual degree of isostatic compensation in the region, rather than theoretical conditions. Subsidence or uplift data alone cannot provide this to facilitate the geophysical interpretation of MQ equations; an interaction with classical isostatic procedures must be established. Direct correlation studies of the relationship of differential crustal movement with changes in the gravity anomaly in the same time period would also be useful.

Having discussed the need for using topographic heights and gravity data in future tests, we now return to a question discussed briefly in a previous section. In particular, the validity of using eqs. (39) and (43) to fit topographic subsidence velocities needs to be established. As given, their proper application appears to be limited to the rate of change of disturbing potential with time. With a simple modification, these equations are also relevant to crustal velocities because disturbing potential is related to small height changes by a linear proportionality. Bruns' formula, $N = T\gamma$, is a well known demonstration of this fact because N is a geometric height separation of the geoid and a standard ellipsoid; T is disturbing potential; and γ is a standard gravity value, namely the proportionality constant.

Taking N and T as dependent variables, and γ as a constant, we partially differentiate with respect to time to obtain $\partial N/\partial t = \gamma^{-1}\partial T/\partial t$. We may re-express this as $\partial H/\partial t = \gamma_t^{-1}\,\partial\tau/\partial t$ for our particular case. The term $\partial H/\partial t$ is topographic subsidence with respect to time. Thus, $\partial H/\partial t$ corresponds conceptually to $\partial N/\partial t$ in terms of a small height separation with time. The term τ is a potential difference at the level of the topographic surface, corresponding conceptually to disturbing potential T at ellipsoid level. The term γ_t is still standard gravity, but if the topographic height is large we may want to adjust it to topographic level. Using this relationship, we are justified in re-expressing the relationships in eqs. (39) and (43) in the form

$$\frac{G}{\gamma_t}\sum_{j=1}^{n}\omega_j\left[\left(X-X_j\right)^2+\left(Y-Y_j\right)^2+\delta^2\right]^{-1/2}=\frac{\partial H}{\partial t}=V(X,\,Y). \qquad (45)$$

Equations (40) and (42) may also be expressed as

$$\frac{G}{K} \sum_{j=1}^{n} \omega_j \left[\left(X-X_j\right)^2 + \left(Y-Y_j\right)^2 + \delta^2 \right]^{1/2} = \frac{\partial H}{\partial t} = V(X, Y). \qquad (46)$$

Thus, we have established a form of theoretical equivalence of the reciprocal hyperboloid and hyperboloid kernels for predicting vertical crustal velocities under certain restricted conditions. The results in Table 2 have already established the practical equivalence.

Given the same data sets, both types of kernels and their associated coefficients respond as needed to give an unusually good surface fit. The kernels are different and the coefficients are different (in the sense that $G\,\omega_j/\gamma_t \neq G\omega_j/K$ in general), yet the sums of their respective products at any given evaluation point result in uncannily similar predictions.

Equation (45) should be considered the most reliable for isolating the actual time rate of change of the point mass anomalies because the quantity γ_t is relatively well known, whereas K is not. For the present, it is tentatively assumed that K is a single constant for a region, but it may turn out that there is a K_j for each point mass anomaly. Because K seems to be dependent, in any case, upon each actual topographic height and upon the degree of isostatic compensation rather than upon a differential change in height, it is important to use more detailed data in future tests. As previously mentioned, both gravity anomalies and actual topographic information associated with subsidence or bulge topography are needed to assist in quantifying the so-called K factor. With sufficient refinement, eq. (46) should complement the usefulness of eq. (45), and together support a more complete geophysical interpretation of the mass redistribution associated with crustal movements.

CONCLUSIONS AND RECOMMENDATIONS

The basic conclusions reached as a result of this investigation are

(1) MQ equations, both harmonic and nonharmonic, are suitable as geometric prediction functions associated with crustal movement studies.

(2) MQ equations have the potentiality for usage in interpreting mass redistribution associated with crustal movements in a mascon anomaly form.

(3) More data are needed for future studies to develop the full potential, and limitations, of mascon anomaly models.

It is recommended that:

(1) The computer programs used in this study (not a part of this report) be documented and filed for future use in crustal movement studies.

(2) Investigations of this type be continued for studies of crustal movement.

(3) Data for future crustal movement studies by geodesists should include detailed gravity and topographic information in addition to the topographic bulge or subsidence information provided by geodetic leveling.

ACKNOWLEDGMENTS

The author is indebted to Dr. John D. Bossler, Captain, NOAA Corps and deputy director of NGS, for suggesting the topic of this investigation and for many helpful discussions. An expression of appreciation is also due to Capt. Leonard S. Baker, the NGS director at the time of this study; Patricia Gaborski, who provided programming support; and all the members of the NGS staff who assisted in making my visit both enjoyable and, from my point of view, very productive.

REFERENCES

Hardy, R. L., 1971: Multiquadric equations of topography and other irregular surfaces. *Journal of Geophysical Research* 76, 1905-1915.

Hardy, R. L., 1972: The analytical geometry of topographic surfaces. *Proceedings of the American Congress on Surveying and Mapping*, 32, 163-181.

Hardy, R. L., 1976: Geodetic applications of multiquadric equations. ERI Project 1070-S, Iowa State University, Ames 85 pp. (NTIS PB 255296).

Hardy, R. L., 1977: Least squares prediction. *Photogrammetric Engineering and Remote Sensing* 42 (4), 475-492.

Hardy, R. L., and Göpfert, W. M., 1975: Least squares prediction of gravity anomalies, geoidal indulations, and deflections of the vertical with multiquadric harmonic functions. *Geophysical Research Letters* 2 (10), 423-426.

Heiskanen, W. A. and Moritz, H., 1976: *Physical Geodesy*, W. H. Freeman and Company, San Francisco, 364 pp.

Hirvonen, R. A., 1971: *Adjustment by Least Squares in Geodesy and Photogrammetry*. Ungar, N.Y., 261 pp.

Holdahl, S. R., 1975: Models and strategies for computing vertical crustal movements in the United States. *Proceedings of the International Symposium on Recent Crustal Movements*, International Union of Geodesy and Geophysics, Grenoble, France, Sept. 2-6, 10 pp.

Holdahl, S. R., 1977: Recent elevation change in southern California. *NOAA Technical Memorandum NOS NGS-7*, National Oceanic and Atmospheric Administration, U.S. Department of Commerce, Rockville, Md., 19 pp. (NTIS PB 265940).

Holdahl, S. R. and Hardy, R. L., 1977: Solvability and multiquadric analysis as applied to investigations of vertical crustal movements. *Proceedings of the 1977 International Symposium on Recent Crustal Movements*, Palo Alto, Calif., July 26 in *Tectonophysics* (in press).

Kearsly, W., 1977: Estimation of anistropic characteristics of gravimetric fields. Paper presented at the Spring Annual Meeting of the American Geophysical Union, Washington, D.C., June 3, 17 pp.

Lauritzen, S. L., 1973: The probabilistic background of some statistical methods in geodesy. Geodetic Institute, Meddelese No. 48, Copenhagen, 96 pp.

Miller, K. S., 1963: *Engineering Mathematics*, Dover Publications, N.Y. 417 pp.

Moritz, H., 1972: Advanced least-squares methods. Department of Geodetic Science Report No. 175, Ohio State University, Columbus, 128 pp.

Moritz, H., 1976: Least-squares collocation as a gravitational inverse problem. Department of Geodetic Science Report No. 249, Ohio State University, Columbus, 28 pp.

Scheid, F., 1968: *Theory and Problems of Numerical Analysis*. McGraw Hill, N.Y., 422 pp.

Yaglom, A. M., 1962: *An Introduction to the Theory of Stationary Random Functions*. Prentice Hall, Inc., Englewood Cliffs, N.J., 235 pp.

(Continued from inside front cover)

NOS NGS-6 Determination of North American Datum 1983 coordinates of map corners. T. Vincenty, October 1976, 8 pp (PB262442). Predictions of changes in coordinates of map corners are detailed.

NOS NGS-7 Recent elevation change in Southern California. S.R. Holdahl, February 1977, 19 pp (PB265-940). Velocities of elevation change were determined from Southern Calif. leveling data for 1906-62 and 1959-76 epochs.

NOS NGS-8 Establishment of calibration base lines. Joseph F. Dracup, Charles J. Fronczek, and Raymond W. Tomlinson, August 1977, 22 pp (PB277130). Specifications are given for establishing calibration base lines.

NOS NGS-9 National Geodetic Survey publications on surveying and geodesy 1976. September 1977, 17 pp (PB275181). Compilation lists publications authored by NGS staff in 1976, source availability for out-of-print Coast and Geodetic Survey publications, and subscription information on the Geodetic Control Data Automatic Mailing List.

NOS NGS-10 Use of calibration base lines. Charles J. Fronczek, December 1977, 38 pp (PB279574). Detailed explanation allows the user to evaluate electromagnetic distance measuring instruments.

NOS NGS-11 Applicability of array algebra. Richard A. Snay, February 1978, 22 pp (PB281196). Conditions required for the transformation from matrix equations into computationally more efficient array equations are considered.

NOS NGS-12 The TRAV-10 horizontal network adjustment program. Charles R. Schwarz, April 1978, 52 pp (PB283087). The design, objectives, and specifications of the horizontal control adjustment program are presented.

NOS NGS-13 Application of three-dimensional geodesy to adjustments of horizontal networks. T. Vincenty and B. R. Bowring, June 1978, 7 pp (PB286672). A method is given for adjusting measurements in three-dimensional space without reducing them to any computational surface.

NOS NGS-14 Solvability Analysis of Geodetic Networks Using Logical Geometry. Richard A. Snay, October 1978, 29 pp. No algorithm based solely on logical geometry has been found that can unerringly distinguish between solvable and unsolvable horizontal networks. For leveling networks such an algorithm is well known.

NOAA Technical Reports, NOS/NGS subseries

NOS 65 NGS 1 The statistics of residuals and the detection of outliers. Allen J. Pope, May 1976, 133 pp (PB258428). A criterion for rejection of bad geodetic data is derived on the basis of residuals from a simultaneous least-squares adjustment. Subroutine TAURE is included.

NOS 66 NGS 2 Effect of Geoceiver observations upon the classical triangulation network. R. E. Moose and S. W. Henriksen, June 1976, 65 pp (PB260921). The use of Geoceiver observations is investigated as a means of improving triangulation network adjustment results.

NOS 67 NGS 3 Algorithms for computing the geopotential using a simple-layer density model. Foster Morrison, March 1977, 41 pp (PB266967). Several algorithms are developed for computing with high accuracy the gravatational attraction of a simple-density layer at arbitrary altitudes. Computer program is included.

NOS 68 NGS 4 Test results of first-order class III leveling. Charles T. Whalen and Emery Balazs, November 1976, 30 pp (GPO# 003-017-00393-1) (PB265421). Specifications for releveling the National vertical control net were tested and the results published.

NOS 70 NGS 5 Selenocentric geodetic reference system. Frederick J. Doyle, Atef A. Elassal, and James R. Lucas, February 1977, 53 pp (PB266046). Reference system was established by simultaneous adjustment of 1,233 metric-camera photographs of the lunar surface from which 2,662 terrain points were positioned.

NOS 71 NGS 6 Application of digital filtering to satellite geodesy. C. C. Goad, May 1977, 73 pp (PB-270192). Variations in the orbit of GEOS-3 were analyzed for M tidal harmonic coefficient values which perturb the orbits of artificial satellites and the Moon.

NOS 72 NGS 7 Systems for the determination of polar motion. Soren W. Henriksen, May 1977, 55 pp (PB274698). Methods for determining polar motion are described and their advantages and disadvantages compared.

(Continued on inside back cover)

*U.S. GOVERNMENT PRINTING OFFICE: 1978 281-067/350 1-3

(Continued)

NOS 73 NGS 8 Control leveling. Charles T. Whalen, May 1978, 23 pp (GPO# 003-017-00422-8) (PB286838). The history of the National network of geodetic control, from its origin in 1878, is presented in addition to the latest observational and computational procedures.

NOS 74 NGS 9 Survey of the McDonald Observatory radial line scheme by relative lateration techniques. William E. Carter and T. Vincenty, June 1978, 33 pp (PB287427). Results of experimental application of the "ratio method" of electromagnetic distance measurements are given for high resolution crustal deformation studies in the vicinity of the McDonald Lunar Laser Ranging and Harvard Radio Astronomy Stations.

NOS 75 NGS 10 An algorithm to compute the eigenvectors of a symmetric matrix. E. Schmid, August 1978, 5 pp. Method describes computations for eigenvalues and eigenvectors of a symmetric matrix.

NOS 76 NGS 11 The application of multiquadric equations and point mass anomaly models to crustal movement studies. Rolland L. Hardy, November 1978, 55 pp. Multiquadric equations, both harmonic and non-harmonic, are suitable as geometric prediction functions for surface deformation and have potentiality for usage in analysis of subsurface mass redistribution associated with crustal movements.

U.S. DEPARTMENT OF COMMERCE
National Oceanic and Atmospheric Administration
National Ocean Survey
National Geodetic Survey, C13x4
Rockville, Maryland 20852

OFFICIAL BUSINESS

POSTAGE AND FEES PAID
U.S. DEPARTMENT OF COMMERCE
COM-210
THIRD CLASS MAIL